DEVELOPMENT OF AN APPROPRIATE, LOW-COST SOLAR-POWERED STIRLING MOTOR FOR WATER PUMPING

P Wagner • CJ Rallis • AE Bunn • PA Heimann
G Walker • BM Mangaya

WRC Report No 875/1/00

Water Research Commission

DEVELOPMENT OF AN APPROPRIATE, LOW-COST, SOLAR-POWERED STIRLING MOTOR FOR WATER PUMPING

P Wagner ■ CJ Rallis ■ AE Bunn ■ PA Heimann ■ G Walker ■ BM Mangaya

REPORT TO THE WATER RESEARCH COMMISSION

by

WAGNER SYSTEMS

WRC Report No 875/1/00
ISBN 1 86845 704 4

CONTENTS

EXECUTIVE SUMMARY	**3**
INTRODUCTION	3
RESULTS	4/5
CONCLUSION AND RECOMMENDATIONS	6
ACKNOWLEDGEMENTS	**7**
INTRODUCTION	**8**
STIRLING BROTHERS	9-15
INTRODUCTION CONTINUED	16/17
LITERATURE REVIEW	**19**
LOW DELTA T STIRLING ENGINES	19-21
SYSTEM DESIGN	**22**
ENERGY CONSIDERATIONS	22
DESIGN CONSIDERATIONS	23
MATERIALS	24
INNOVATION	24
MEMBRANE AND OUTPUT SHAFT DRIVE	25
SOLAR ENERGY CONVERSION	26
SPECIFICATIONS	26
SELF STARTING SYSTEMS	27
CONCLUSION AND RECOMMENDATIONS	**28**
REFERENCES	**29**

EXECUTIVE SUMMARY

INTRODUCTION

In the development of any rural community, social upliftment and infrastructure development are of significant importance. These elements and others have to be addressed within the context of the environment and the socio-political situation of the community.

Ideally, projects need to be developed that address more than one area of interest. This multi-sectoral approach not only increased the effectiveness of rural community development but also enhances the cost-effective nature of the project. Improved water supply by making use of solar energy is indeed such a project.

This project has attempted to address the above by integrating a unique method of energy conversion with appropriate technology transfer in order to develop a low-cost solar water pump.

Although, climatic conditions are good for using solar power in much of the developing regions in Africa, the cost and the complexity of existing systems have generally prevented their successful implementation. It is however, this aspect of cost, relative simplicity and appropriateness that makes the developed solar powered Stirling motor unique. Special emphasis has been given to:

- cost - initially plastic standard material was envisaged and used, however most of these degraded rapidly in outdoor and sun exposed climatic condition (mainly by changing shape). The replacement of these by using glass and metal did not increase cost to any great extent but improved the quality substantially.
- avoiding technical complexity - the adopted design is void of any complexity.
- sustainability - no material was used which is more standard it could not be procured in the future.

The primary objective of the project were to:

(i) develop and construct a low-cost and appropriate solar powered (Stirling) motor and for integration to a water pump.

(ii) optimise the solar pump design and construction process so as to ensure that conditions present in developing countries and rural areas are not inhibiting to this technology.

(iii) to optimise the efficiency of the motor

(iv) to test, evaluate and assess the solar motor and pump in a rural setting

RESULTS

Positive

A low cost Stirling motor has been designed and built. The low delta-T design (working between 30-70°C) has a solar radiation collecting area of 2 X 3m². This system does not rely on parabolic dishes or solar concentrators nor tracking system. The problems encountered in scaling up to a motor of this size have required the incorporation of some novel features. These innovations include:

i. A solar electric pumping system for air which increases the air pressure inside the motor before starting by 7- 10 millibar above ambient

ii. A solar electric self starter which ones working pressure is achieved starts the solar motor by working the regenerator assembly during sunshine e.g. solar radiation exposure.

iii. A 3m² glass window sealed by a membrane hinged on one side is used as the power output piston.

iv. A output shaft system whose rate of turn is proportional to rise and fall movement of the glass window piston.

v. The glass window piston can be loaded with weights to adjust to any working pressure above ambient - e.g by loading 100kg per window piston = 10 millibar.

vi. The continuos positive air pressure during the working cycle reduced the flexing of the casing and membrane.

vii. The two solar window acting as pistons are raised and lowered alternatively every second. These pistons carry a load of 100kg each and avoiding a flywheel their drop energy can be used to turn the output shaft or work a pump. Total movement of each window is between 12 to 25mm depending on the incline of the sun.

Pit Falls

(i) Sealing - The large size of the engine is difficult to seal for air losses, to minimise this loss requires more expensive material and workmanship. The demand for this increases with the higher positive air pressure inside the motor.

(ii) The large solar collector regenerator which is $3m^2$ in size limits, because of its weight, the speed e.g rate by which it can be moved. The rate of 1HZ seems the maximum due to inertia forces, however a faster rate would increase the output.

(iii) The required strength of the solar window frame impedes e.g. reduces solar radiation to reach the regenerator.

CONCLUSIONS AND RECOMMENDATIONS

The following conclusions are reached:

(i) A large scale low-cost Stirling motor of the low delta-T type (30-70°) seems too inefficient for solar energy conversion due to the inertia limited low operating speed which does not exployed the energy fully which the regenerator receives.

(ii) The flexing losses of the large components could only be suppressed by more expensive materials and design features.

(iii) Positive pressure inside the motor through continuous trickle feed pumping does to an extent reduce the flexing losses and increase the output

(iv) Reflextive losses at lower solar radiation angles are too pronounced and unavoidable.

(v) The low temperature gap 30-70° C proved too narrow to exploit for a cost effective conversion of solar energy for water pumping. It is recommended and our conclusion that the engine delivers insufficient power to warrant further work, and as a result the project should be closed. Nevertheless, much investigative and innovative work has been carried out. I think it is important to document this in such a way that future researches in this area can learn from the work carried out.

ACKNOWLEDGEMENTS

The research in this project emanated from a project funded by the Water Research Commission (WRC) and entitled;

DEVELOPMENT OF AN APPROPRIATE, LOW-COST, SOLAR-POWERED STIRLING MOTOR FOR WATER PUMPING

The steering committee responsible for this project, consisted of the following persons:

Mr DS van der Merwe, WRC

Mr AG Reynders - WRC (deceased)

Mr JN Bhagwan - WRC

Dr D Banks - University of Cape Town

Mr A Brink - Green Energy Systems

Mr HC Chapman - Cape Metropolitan Council

Mr C Chibi - Mvula Trust

Mr J Fuls - Institute for Agriculture Engineering, Agricultural Research Council

Mr P Janse vRensburg - Green Energy Systems

Mr CS Crawford - Department of Water Affairs and Forestry

Prof CJ Rallis - University of the Witwatersrand

Mr P Wagner

The financing of the project by Water Research Commission and the contribution of the members of the Steering Committee is gratefully acknowledged.

The project was only possible with the co-operation of many individuals and institutions. The authors therefore wish to record their sincere thanks to the following:

Mr T Henke

Brits Textile Products

Mr A van Rooyen

Mr D. Esterhuyse - Weather Bureau

INTRODUCTION

The invention of an external combustion engine or hot air engine dates back to 1815 when the brothers James and Robert Stirling of Glasgow filed a portend which came to be known as the stirling engine - or the stirling principle. This type of engine was used to pump water from coalmines. I have taken the liberty to include the following 7 pages from a book by my friend Ivor Kolin for Dunbroonik for the purpose to gain understanding of the principle of the invention.

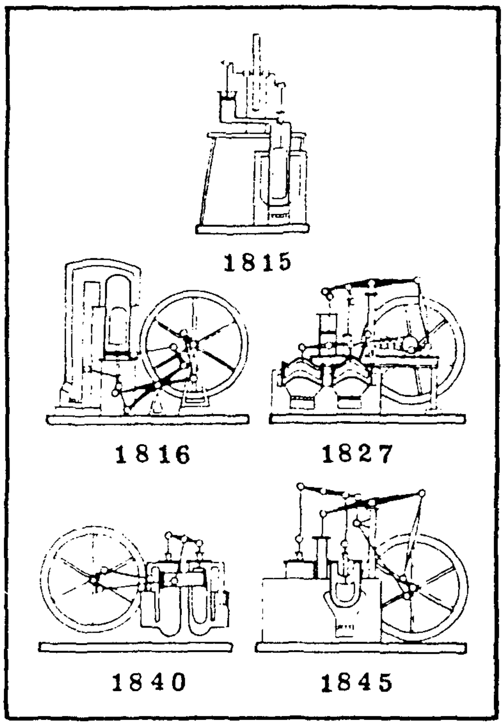

2

STIRLING BROTHERS

The inventor was not a minister but an engineer, the invention was not a single engine, but five variants of the same working principle, and finally, the ideal Stirling cycle has never been realised.

In modern literature the invention of the Stirling engine is generally attributed to Robert Stirling, which may be attractive, but it is rather doubtfull. There are in fact numerous indications in favour of his brother James.

Historically , both brothers : Robert Stirling , Minister of Galston and James Stirling, Engineer in Glasgow, signed their patent applications together. In spite of this, brother James was later unjustifiably ommitted in the contemporary sources.

The only written sign that Robert was engaged on the Stirling engine is his name, together with his brother James´ on the patent specifications. Of course this can not be sufficient to evaluate Robert´s technical contribution. That was the initial reason for Mr.Edelman from the Philips Co. to under- 35
take an extensive exploration voyage to find more technical proofs in the favour of brother Robert.

First of all, Edelman visited Science Museum in London, in- 107
cluding its unique library and the world famous British Museum Library as well. He also discussed the matter with professional people from the Newcomen Society for the Study of the History of Engineering and Technology in the headquarters of the Society. Needless to say he visited University of Glasgow and Cloag, Stirling´s birthplace, as well as many other places where Stirling lived.

At the end of hise extensive research (1969), Edelman wrote that he had learned a lot about Scottish life and habits and enjoyed a real Scottish tea with bacon and eggs. Nevertheless, he found no written proof for Robert's technical contribution.

Edelman found out thet Robert had been born in 1790 and in 1806 he studied Advanced Latin and Greek. He was licensed to preach in 1815 and became Minister of the Church at Galston in 1824. The University of St.Andrews conferred upon him the honorary degree of Doctor of Divinity in 1840. When the scourge of cholera came to Galston, Dr.Stirling fearlessly moved among the plaque-stricken homes and parish. He ministered faithfully of the physical and spiritual wants of the sufferers and toiled among them night and day. The history of Galston Perish Church records Dr.Stirling as a Christian hero who died in 1878, aged 88, in the 53rd year of his ministry.

According to the above quoted documentation, brother Robert, Doctor of Divinity , deserved a great merit as the distinguished Minister of Galston.

On the other hand, his brother James, engineer, may be considered a real inventor of the hot-air engine. That may be recognised from many technical papers. In the first place here is the large report, written by James Stirling himself, published in the Proceedings Institution Civil Engineering in June 1845 (pp.348-61).

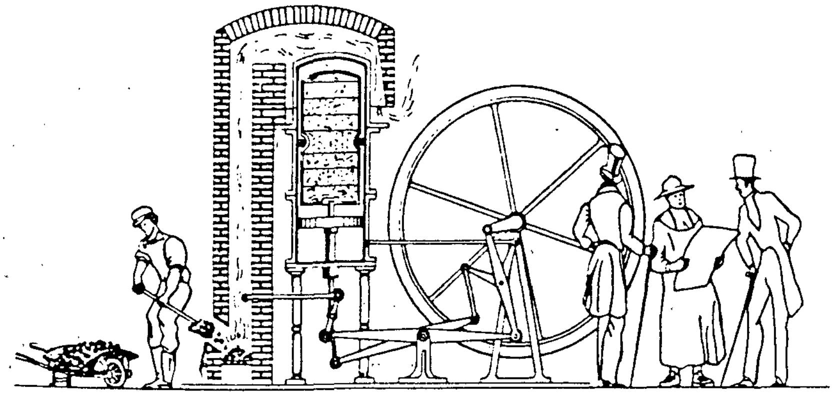

It is enough to read this highly professional document to obtain a clear picture about James'thermodynamical knowledge and mechanical capabilities.

As a contrast to this, it is hard to believe that Dr.Robert Stirling, who was completely engaged in his respectable work was in position to be continuously active in the engineering field at the same time.

Technical research and development process requires a full engagement of the complete person. In other words somebody must work exclusively night and day to solve ceaselessly arising new problems, caused by numerous technical details.

Moreover , indispensable thermodynamical and mechanical knowledge is unavoidable at least for the calculation of heat exchanger, even under the supposition that the main conception is good.

Generally speaking, an idea alone does not constitute an invention, even if it is supposed to have been Robert´s. In this respect the renowned German magazine "Dingler´s Polytechnisches Journal" wrote :

"The real inventor in our sense remains the man who not only conceived some idea, but carried it out to its successful end." (1876, Bd. 220, S.187)

The same opinion was expressed in another form by professor Robinson from England , who also said that only a good idea was not sufficient for an invention :

"This should teach the future inventors the lesson to stick to a good idea and make it practical success rather than merely resting satisfied with the notion it is good."

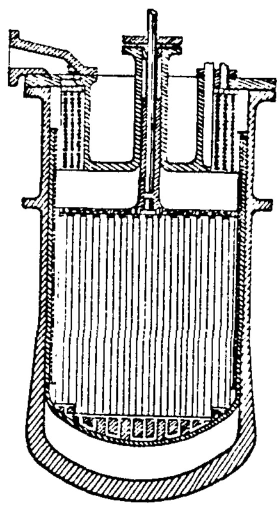

Furthermore , practical realisation of the initial idea requires additional workshop drawings and assembly drawings. Numerous technical designs could only have been made by a specialist like James, the engineer. That may be seen throughout all the three Stirling patent specification :

No 4081 / 1816

No 5456 / 1827

No 8652 / 1840

The next argument for James originates from the test report on the Stirling engine (1854) when eleven eminent experts of that time were present, among them Sir John Renie, President in the Chair of Mechanical Engineers,Sir George Cayley,Robert Stephenson and others.Only James of the Stirling brothers was present, who as an engineer, was able to explain the theory and answer the question of the commission.

Consequently, brother James was the right one who practically developed the new engine including numerous technical details. As a final result, James confirms initial theoretical assumptions by starting in practice the first hot-air engine "on a principle entirely new." Having all this in mind, it may be concluded on the ground of the historical papers and documents, that James Stirling, engineer in Glasgow, deserved a merit to be confirmed as the real inventor of the Stirling engine.

The exhibit has a long vertical cylinder containing air which is heated by an external source. A long and loosely fitting displacer works within this cylinder, it is made of thin metal and is operated by means of an overhead crankshaft with flywheel.

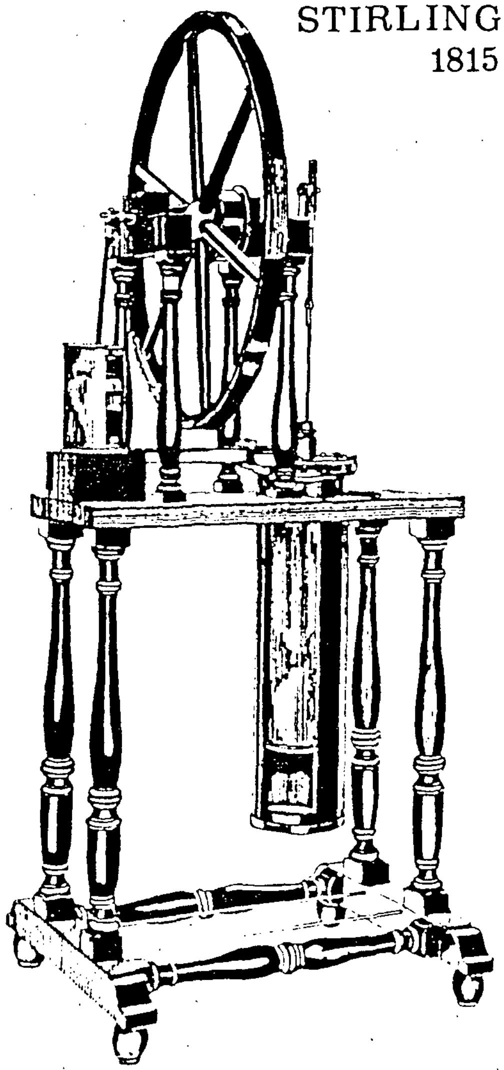
STIRLING
1815

At the opposite end of the crankshaft there is another crank which operates the working piston in a separate cylinder. The bottom of this cylinder communicates with the top of the displacer-cylinder through a pipe. Its working piston is packed with a double cup-leather and its crank is set 90° behind the displacer crank.

EDINBURGH :- This is a sectioned copy of a model which is preserved in the University of Edinburgh and is believed to have been the earliest model made about 1815.

"The included air is brought to the warm part of the cylinder has its elasticity increased and presses upon the piston with a force greater than that of atmosphere. The piston is thus forced downwards till the pressure of the included air and that of atmosphere become equal."

"The impulse communicated to the fly carries the end of the crank , and the arm and bent lever are brought to such a position as to depress the rod and thus to raise the plunger from the piston."

"The included air is thus made to descend between the plunger and cylinder and brought to the cold part; it is cooled in its descent, has its elasticity diminished, and its pressure becomes less than that of the atmosphere, the piston is forced upwards, and the crank downwards."

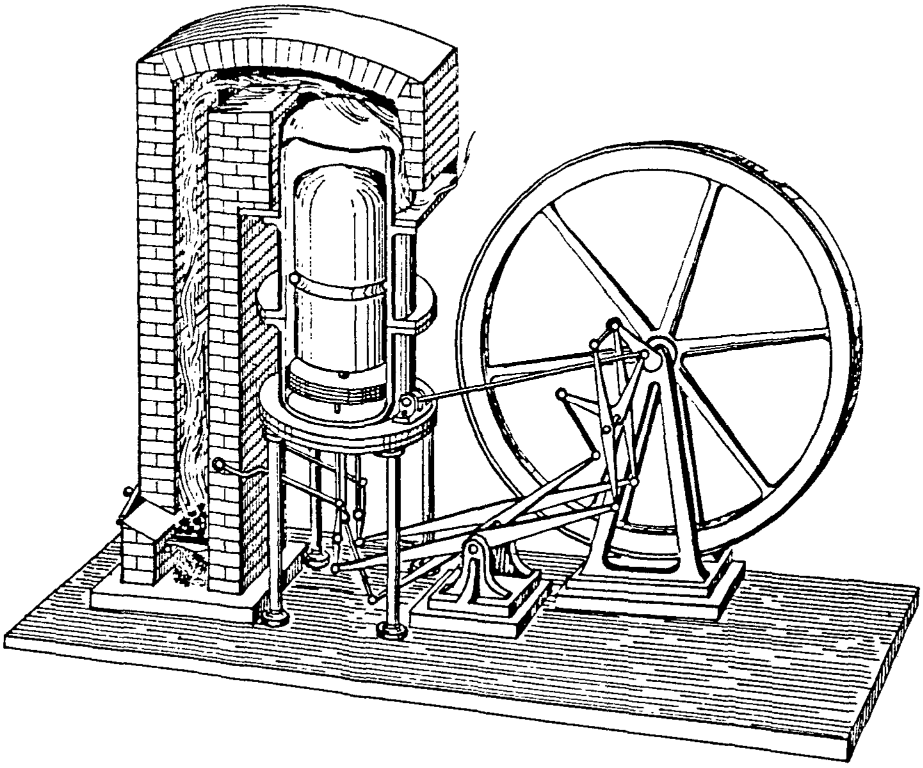

"The revolution of the fly and crank again bring the plunger towards the piston, the air ascends through the same passage by which it descended, is heated in its ascent and forces the piston downwards and the crank upwards, and so on alternately. In this manner a rotatory motion is produced which may be applied to the moving of machinery."

ROBERT STIRLING: "Improvements for diminishing the consumption of fuel, and in particular an engine capable of being applied to the moving machinery on a principle entirely new."-British Patent No.4081 / A.D.1816.

The first description of regenerator

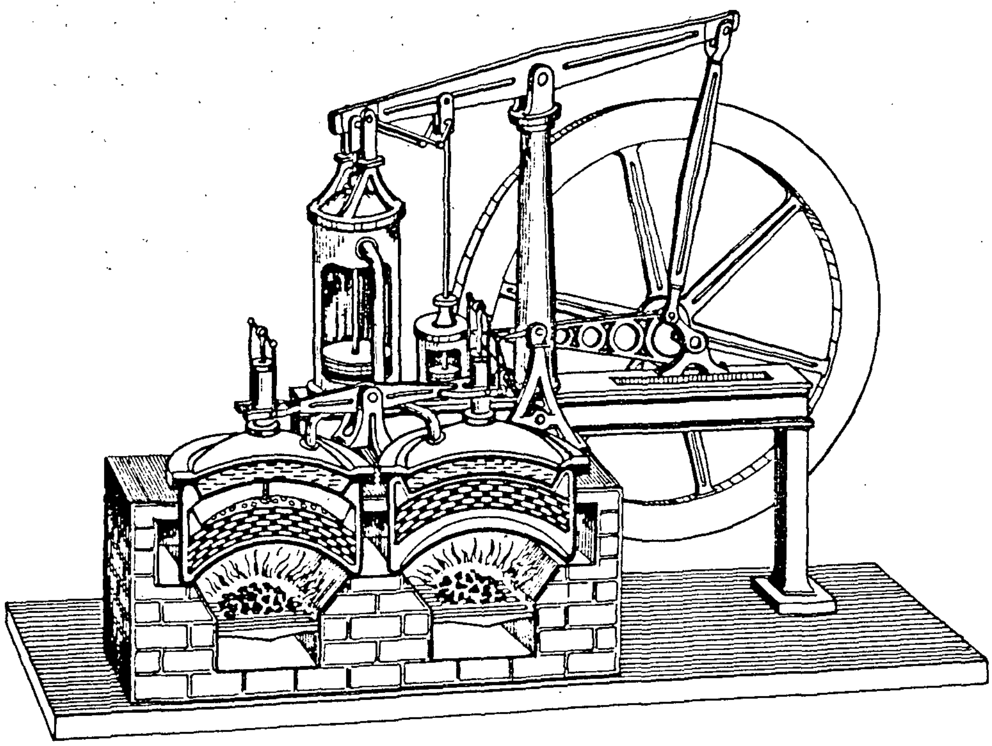

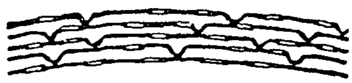

"The space is filled up with successive layers of plates of the thinnest iron in use, pierced with holes, as already described, stamped or hammered into a spherical form, and kept at the distance of two or three times their own thickness from one another by small indentations formed in the inperforated parts by a proper punch or die."

"A vertical section of a small portion of these plates, represent the nature of the said indentations, and also the holes already described . The holes which are made in these thin plates are arranged in rows at equal distances from one another, and each successive layer is so placed that its holes shall not be opposite to those of the layer beneath it. The object of this arrangement is to spread the air more completely over the plates in passing upwards and downwards, and to heat and cool it more effectually."

ROBERT AND JAMES STIRLING: "Air Engines" - British Patent No. 5456 / A.D.1827

STIRLING PRINCIPLE

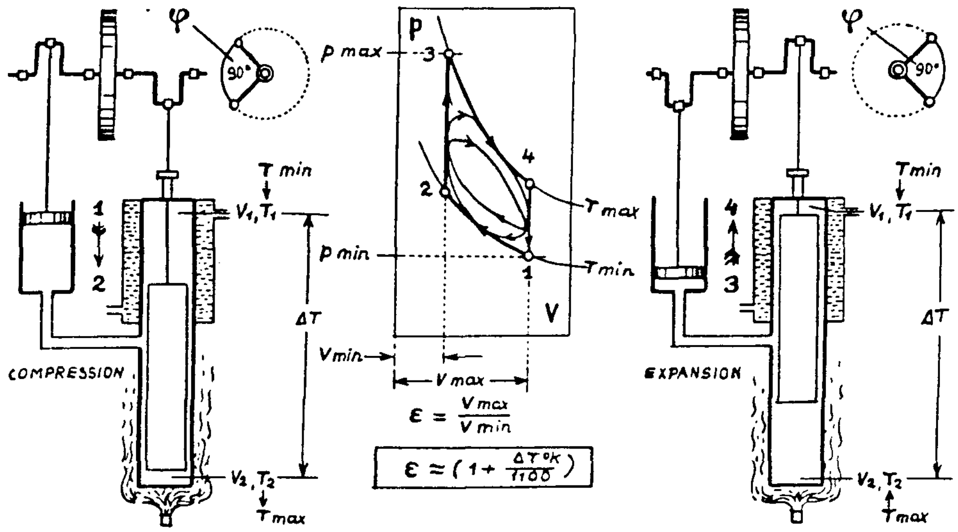

The first Stirling engine,introduced by brothers Stirling, was also the simplest and may be taken as a school example to illustrate the working principle,which is grounded on the simultaneous heating and cooling of a long metal cylinder.

- The motor consists of two cylinders, with two pistons which are moving under a phase difference ($\Delta\varphi$) of about 90°
- The working piston is placed in the smaller working cylinder.
- The long piston in the long cylinder is substantially not a piston, it is called displacer and works as a heat exchanger.
- Diameter of a long displacer piston is for about 1 % smaller than cylinder diameter.Through this narrow annular space, the displacer piston moves the air from the cold to the hot space and vice versa.

Compression : While the displacer piston is situated in the lower part of the cylinder, the entire quantity of air is in the cold space. In this moment the cold air is compressed by the working piston.

Expansion : While the displacer piston is situated in the upper part of the cylinder, the total quantity of the air is in the hot space. In this moment the expansion of the hot air drives up the working piston.

Work or energy : As the expansion of the hot air gives more work than it is spent by compression of cold air the surplus is the useful work on the working shaft.

Due to the influence of the dead space and sinusoidal pistons motion, the actual indicator diagram is rounded and smaller than it should be according to the isothermal cycle.

Introduction continued

1. The aim of this project was the research and development of a solar-powered low temperature difference Stirling engine with a specific application in the field of water pumping.
2. The water pump was to be a self-starting unit that is simple and easy to use, virtually requiring no maintenance, and made of locally available materials, thereby ensuring that the low deltaT Stirling engine could in principle easily be fabricated by non-professionals.
3. The water pump was to be driven by a low temperature-difference (deltaT) Stirling engine energised from the heat received via a flat-plate solar collector (regenerator). No parabolic dish or any other solar heat concentrator nor solar tracking system normally associated with solar systems was to be used.
4. The work reported here is based on earlier research and development on low deltaT Stirling engines and models developed by Wagner Systems Ltd., and published the Unesco Journal of Environment and Pollution Volume 6 1996, as well as at the 8th International Stirling Engine Conference in Ancona Italy 1997.
5. Although the application was intended for developing countries and may appear to be of low technological sophistication, the reverse is the case. The low deltaT Stirling engine described in this report is technologically advanced it is derived from novel research and development previously conducted by Wagner Systems.
6. Low deltaT Stirling engines have been described and published before. The theory of Stirling engines has been well summarised by Kolin (1989), Senft (1995), Walker et l.c. (1994) and by Rallis (1997).

7. Recent developments in the low deltaT Stirling engine environment have resulted in Stirling machines being able to operate on small temperature differences (less then 100°C between the hot and cold space; Kolin (1989) and Senft (1995). These developments have ensured that Stirling engines now are able to use flat plate solar collectors to work efficiently. There is thus no longer the need for parabolic solar concentrators, absorbers and tracking systems used in conventional solar powered Stirling systems.
8. In addition, low deltaT Stirling engines which operate at temperatures less than 100°C eliminate the need for expensive and specially machined parts. Instead low cost, locally available materials may be used and village craftsmen may make the machines by using pre-manufactured components (those items outside their capability of craft) but making the simple items and doing the assembly.

The primary objectives of the project were:

- The development and construction of a low-cost and appropriate Stirling motor and integrated water pump.
- The prototyping and design of this technology and the optimisation of the efficiency of the motor.
- Testing, evaluation and assessment of the solar motor and pump in a rural setting.
- The optimisation of the solar pump design and construction process to ensure that conditions present in developing countries and rural areas are not inhibiting to this technology. These will include the optimisation of cost, appropriateness, sustainability and technical complexity.

The Stirling Engine

The internal combustion engine denies power from the expansion of burning fuel inside the cylinder of the engine.
The external combustion engine e.g. STIRLING ENGINE exploits the transfer of heat from a hot part to a cooled part of its casing via a REGENERATOR.
A regenerator is: any filter material which imposes its state of heat upon the passing gas. Shown below : a regenerator piston in a cylinder -

Hot Gas Cold Gas Cylinder

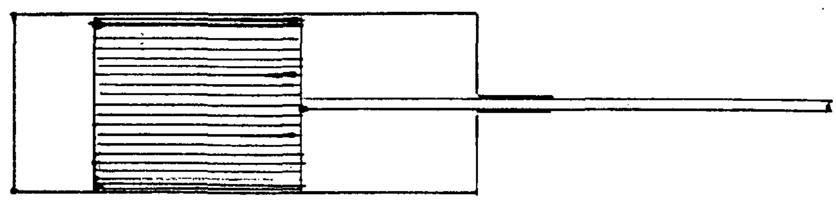

Hot Side Cold Side

Regenerator

sliding to the left e.g. hot end - regenerator absorbs heat from the gas - most gas cooled - pressure decreased
sliding to the right e.g. cold end - regenerator returns heat to the gas - most gas heated - pressure increased.
These gas pressure variations acting in an additional cylinder - piston connected to the aforegoing is a Stirling Engine.

Piston Up

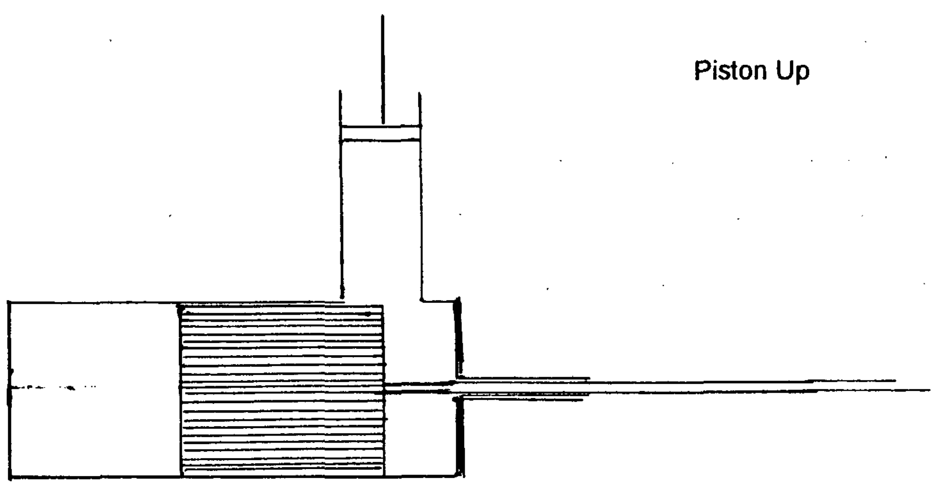

Hot Gas Cold Gas

LITERATURE REVIEW

LOW DELTA T STIRLING ENGINES

1. Stirling engines are a form of heat engine invented in the early 19^{th} century. They enjoyed substantial commercial success until the invention of the electric motor and the internal combustion engine caused the relegation of Stirling engines to a few specialist applications.
2. Low deltaT Stirling engines however, are a relatively recent development and important because they provide the possibility for the use of simple flat-plate solar collectors compared with the complicated, expensive, sun-tracking parabolic collectors used in high performance installations.
3. Various concepts for low delta T Stirling engines that fulfil the above requirements have been investigated and by building small models their validity confirmed.
4. Senft (1995) has recently reviewed and published the history and principal applications of low deltaT Stirling Engines.
5. Most of the experimental work carried out was tested on small model engines. This approach allows new concepts to be rapidly evaluated at little cost and only needs limited infrastructure.
6. The model engine used for most of the experimental work was the *Ringbom*[1]-Stirling engine. The engine was designed by Professor James Senft[2] in the course of his continuing study of low deltaT Stirling engines.

---

1 The New Engine Co. Ltd. Manufacturer of Ringbom

[2]Department of Mathematics and Computer Science, University of Wisconsin, River Falls Wis., USA.*

New Engine Co. Ltd, 12121 NE 66 ST. Kirkland, Washington 98933, USA

7. *Ringbom*-Stirling engines are characterised by the use of a free regenerator and piston assembly which is activated by pressure changes accuring inside the engine using the outside ambient pressure as a base line pressure reference. The power output is via a crank controlled second piston. The technology for Ringbom Stirling engines has been well summarised by Senft (1992).
8. The model of the above described engine is designed to operate with hot water in the reservoir or well in which the engine is operating. The engine can run for several hours on a litre or so of hot water. In this configuration the bottom plate of the regenerator cylinder is the hot plate (at hot water temperature) and the upper plate is the cold plate (at room temperature). It is this temperature difference between the two plates which causes the engine to run.Heat is drawn from the hot water through the hot plate to the air inside chamber.
9. Heat is transferred from the air through the top plate to the environment. Some of the heat entering the engine is converted to work to drive the piston - crank-flywheel assembly.
10. With a solar energy input the hot plate would be the top plate and the cold, air cooled, plate would be underneath. This can be achieved by inverting the engine. Early prototypes by Wagner Systems have shown that the motor is as efficient in this reverse configuration.
11. It was documented (Walker and Senft, 1983) that substantial improvement in performance and great simplification in manufacture, could be gained by converting this machine to the free piston arrangement.
12. Free piston Striling engines are another special class of Stirling engine in which there is no kinematic mechanism connecting the piston and regenerator to each other or to the crankshaft/flywheel assembly.
13. In a free piston Stirling engine there need not be a crankshaft or flywheel. The output work may be taken directly from the piston to drive a linear electric generator, a water pump or gas compressor. The technology of *free piston* Stirling engines has been well summarised by Walker et al. (1997).
14. In the free piston engine described by Walker and Wagner (1997), both the regenerator and the piston, when at rest, are held in the midstroke position by light coil springs,. The springs are

provided simply to support the reciprocating elements in the rest position and to facilitate easy starting. They play little or no part in the operation of the engine when it is running.

15. Free piston Stirling engines operate at their natural frequency and are essentially a tuned fluid circuit. Tuned fluid circuits exploit the oscillatory movement of a liquid in a closed U-shaped pipe which is driven by heated gas above the level of the liquid. The rise and fall of the liquid is converted into a pumping action. Both the piston and the regenerator oscillate at the same frequency. The regenerator leads the piston by 90 degrees. When the load conditions or temperature regime change the frequency remains the same but the stroke (principally of the piston) changes to reflect the increase or decrease of work output.
16. Free piston Stirling engines may be used as power systems of refrigerators. In power systems work is taken directly from the reciprocating piston to operate the plunger of a water pump or air compressor. The piston may also cause the oscillation of the armature or the stator of a linear electromagnetic power generator. For small power systems permanent magnets may be used.
17. When Stirling machines are used for refrigeration various arrangements are possible. With electric power available the driver may be a linear electric motor similar to the electromagnetic generator described above. Power input to the conductor coil creates a magnetic field that interacts with the permanent magnets on the piston to create a linear driving force causing the piston to move.

SYSTEM DESIGN

1. Adaption of proven model concepts for the indended practical application of the low deltaT Stirling engine may be categorised into three distinct phases.
   - The research, design and evaluation of the low deltaT Stirling engine with specific emphasis on the optimisation of mechanics, material utilisation and engine efficiency.
   - Implementing of a large scale working prototype, and
   - Optimising the driving mechanism for a pump.

2. The research and development leading up to the present low deltaT Stirling engine is based on the evaluation of a number of different low deltaT Stirling engine models. These systems where designed and constructed to evaluate various aspects of the low deltaT Stirling engine in particular, issues related to the engine performance and material selection.

Energy Considerations

3. deltaT is defined as a temperature difference between the hot and cold sections of the low deltaT Stirling engine and in our case not greater that 35°C and often less.
4. Such a small temperature difference limits the thermal efficiency of the engine to quite a low value. Theoretically the *Carnot* efficiency could be 10 percent for such a system but in practice is probably nearer to 5%.
5. The solar constant e.g. the amount of solar radiation in all spectrum of photon energy (for Cape Town approximately 800 Watts in summer months) outside the earth's atmosphere is 1360 Watts/m². The maximum incident solar energy at equatorial noon is about 1000 Watts/m². Thus, 5 percent if realised, of this energy converts to a theoretical engine output of 50 Watts per square metre of flat plate solar collector. However, this seemingly insignificant output would translate to a flow of 5 kg or 5 litres of water lifted one metre every second or 1800 litres of water lifted 10m every hour per square metre of plate flat collector, provided that the large low deltaT Stirling engine can capture and convert the energy.

Design Considerations

6. The solar powered Stirling engine developed in this project has an innovative arrangement that is unique amoung the low deltaT Stirling engines reported thus far. It consists of two identical assemblies each has a regenerator which acts as the solar energy collector and each measures 2.58 by 1.24m.

7 . Figure 2 (see Appendix A) displays the final assembly of the unit:

   A. Cable to drive regenerator Fig. 1& 2
   B. Drive aluminium beam (swinging beam) Fig. 2
   C. Aluminium frame Fig. 1&2
   D. Glass sheet Fig. 1
   E. Clear PVC membrane Fig. 1
   F. Wooden box (chamber) Fig. 1&2
   G. Guide Rail's for Regenerator H. Fig 1
   H. Regenerator Fig. 1
   I. Wheel to guide regenerator N Fig. 1
   J. Metal bottom Fig.1

8. The two flat plate collectors (regenerators) inside the two Stirling engines are coupled by a swinging beam 'see-saw' arrangement with a 0,14m vertical movement (figure 3).

9. The regenerators are caused to move up and down by a solar driven electric motor or by using already the regenerator to move downward while the regenerator in the other engine is moved upward. This motions switches the directions of the water drive system to the regenerator drive tube associated with the regenerator that was previous elevated. Simultaneously the water in the other regenerator driving tube is released.

10. After a brief interval the regenerator drive tube associated with the elevated regenerator becomes heavier than its opposite twin. This causes the elevated

regenerator to descend and so completing the cycle.

11. As the regenerator reciprocates: A - in the engine chamber it causes cooler air (under the regenerator) to pass through the regenerator, absorb heat and expand. This change in temperature and resulting expansion of air cause a sufficient change in pressure to move (bulge) the membrane (E Fig. 1 & E) - which can be utilised to perform work. B - On the return movement it causes hot air (above the regenerator) to pass through the regenerator, give up the heat and contract.

12. The membrane is covered by a transparent sheet (D Fig.1) secured by hinges (K Fig.3) on the one side and unrestrained on the other side. As the membrane bulges out (with increased internal pressure) it acts on the transparent sheet causing it to lift and rotate at the hinged side (K Fig. 3). The rising and falling cycle of the transparent rigid solar window (C Fig. 3) causes the pump drive shaft to rotate. This is accomplished by means of levers and one-way bearings fitted on the pump drive shaft (S figure 3). The solar window self is loaded by the weight AA Fig. 1 & 3 by size dictates the pressure above ambient e.g. a 100KG load will increase the inside pressure to 10 millibar above ambient while 55KG will give 4 millibar above ambient when the motor is pressurised and start running. Increase internal pressure of the working fluid air decrease flexing losses by having continuos outside force on the casing.

Materials

13. Low prices have been the deciding factors in the selection of materials for the construction. Availability dictated the size and shape of the motor. Therefore the width of Flexible PVC strips as well as Polyurethane sheeting come in certain sizes. The regenerator is made of Polyurethane "FILTREX" a material recommended for moving regenerators.

Innovation

14. This design incorporated 3 new concepts, which are complimentary to the practical requirement of a solar powered motor. These are shown in Figure 3.

15. 1st Avoidance of cam and lever connections between the output shaft and the drive of the regenerator through the use of solar voltaire for the latter's motion. 2nd Multiple strokes of the membrane window piston are required for each complete turn of the output shaft (S).

16. The drawing (figure 3) explains the design of the output shaft drive (S). The rate of turn is proportional to the available movement from the membrane window piston created by solar radiation as well as output shaft load.

17. Figure 2 shows the solar voltaire panel which drives the airpump (W) and once working pressure working pressure is achieved the motor drive (V) is activated and drives the beam (B) Fig 2&3.

18 . 3rd. Regenerator movement traverses the total height of the chamber. This is achieved by the use of the membrane and window as a piston. Void spaces are therefore reduced which improves

the efficiency of the motor.

19. Figure 2 shows the solar voltaire panel which drives the airpump (W) and once working pressure is achieved the motor drive (V) is activated and drives the beam (B) Fig. 2 & 3.

Membrane and output shaft drive

20 . Figure 3 shows the membrane in the raised position (E) and the low position at point (L), which drive the output shaft. Membranes made of transparent PVC sheeting are a perfect seal for the low deltaT Stirling engine. The membrane (figure 1 (E)) is pressed to the rigid glass sheet (figure (D)) which in turn is attached to the aluminium frame (figure 1 C). This assembly is hinged at point (K) figure 3 in an effort to increase the

movement at the open end where the force is then directed via push rod to the output shaft (S). The alternative rise and fall of the weight, which can be 50-100 by size, advances the shaft via built-in one-way roller bearings at every down stroke..

Solar Energy Conversion

21 . Solar radiation enters the box continuously and heats the upper part of the regenerator. This heating causes the air passing through this regenerator to be heated and to expand. The bottom of the chamber being in contact with a lower temperature medium (e.g. water or soil) keeps the lower half of the regenerator cool.

Specifications

22. Specifications are given below. The low deltaT Stirling engine:

Regenerator chamber

- 2 2.58 x 1.24 meter x 0.2 (w x b x h)
- volume 640 litres

Regenerator

- regenerator 2.57 x 1.23 meter x 0.05m (height)
- 3.2m² pr flat plate collector

Regenerator drive

- 12 W with electric motor powered solar voltaire.

SELF- STARTING SYSTEMS

23. For solar-powered Stirling engines a self-starting device able to start the engine with no human intervention is clearly desirable. The fitted self-start system does activate automatically when the conditions are suitable to accomplish a start.

It also has the capability to reset in the "start" position at sunset or when clouds obscure the sun thereby cooling the engine below operation temperatures.

CONCLUSION AND RECOMMENDATIONS

The following conclusions are reached:

(i) a large scale low-cost Stirling motor has been constructed of simple design

(ii) the motor has been manufactured from easily available standard materials

(iii) the materials were tested and selected first on cost and secondly on suitability

(iv) all problems of the construction have been solved except the following:

(v) the flexing of the chamber bottom - metal base (J) figure 1

(vi) a reduction of flexing was achieved by loading the "SOLAR WINDOW" to 100KG by weight - to force the flexing one directional positive - by increasing the internal working pressure of the motor by 10 millibar

(vii) in spite of this the power output is insufficient e.g. lifting 100kg in 1 sec. 18-25 millimeters high depending on solar strength

(viii) a solar electric motor (V) Fig. 2 has been fitted to start and maintain the movement of the beam

(ix) mathematical modeling indicates that a thinner regenerator material half as thick as the 50 mm at present will increase the output

(x) even an increase to double that is cost-wise not viable

(xi) The low temperature gap 30-70° C is too narrow to exploit for a cost effective conversion of solar energy for water pumping. It is recommended and our conclusion that the engine can deliver insufficient power to warrant further work is valid, and as a result the project should be closed. Nevertheless, much investigative and innovative work has been carried out. I think it is important to document this in such a way that future researches in this area can learn from the work carried out.

REFERENCES

1. Walker G, 1980. Stirling Engines. Oxford University Press. Oxford, UK.
2. Kolin I, 1982. Isothermal Stirling Engines. University of Zagreb. Croatia.
3. Senft L, 1992. Ringbom Stirling Engines. Oxford University Press. Oxford, M
4. Walker G, 1994. Low Capacity Cryogenic Refrigeration. Oxford University Press, Oxford, UK.
5. Beale W, 1995. Private Communication. Stirling refrigerators made by Sunpower,
6. Walker G and Senft L, 1983. Free Piston Stirling Engines. Springer Verlag, New, York, USA.
7. Senft J, 1995. Low Temperature Difference Stirling Engines. Mogriara Press. River Falls, Wisconsin, U.S.A
8. Kolin I, 1989. Stirling Engines: Theory and Practice. University of Zagreb Press. Zagreb, Croatia.
9. Rallis C, 1997 Low Temperature Difference Stirling Engine Development, 1997 8th International Stirling Engine Conference and Exhibition, May 27-30. Faculty of Engineering, University of Ancona, Ancona, Italy
10. Walker G, Wagner PFW, 1997. 8th International Stirling Engine Conference and Exhibition, May 27-30. Faculty of Engineering, University of Ancona, Ancona, Italy
11. Walker G, Reader G, Fanival, D. Bingham ER, 1994. Stirling Engines Gordeon and Breach. Philadelphia, Pennysylvania, U.S.A

A	Regenerator Cable
AA	Weight
B	Drive Aluminium Beam
C	Aluminium Frame and Ribs
CC	Double Sided Rubber Strip
D	Glass
DD	Rubber Seal
E	Membrane
EE	Alumimium Strip
F	Wooden Box (chamber)
G	Regenerator Rail
H	Regenerator
J	Metal Base of Regenerator Chamber
K	Hinge
L	Membrane in Rest Position
M	Sealing Strip
O	Output Shaft
P	Pump Shaft
R	Pump Shaft Lever
S	Drive Shaft
V	Electric Boom Drive Motor
W	Electric Air Pump
X	Membrane in Raised Position
Z	Solar Panel

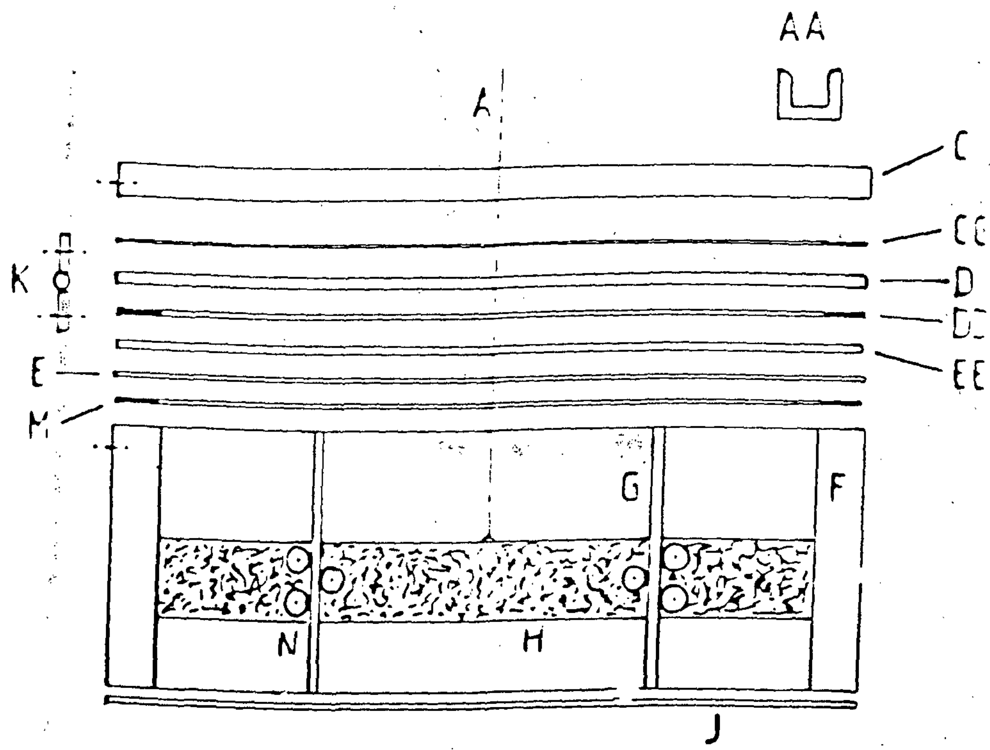

Figure 1

A	Regenerator Cable
AA	Weight
C	Aluminium Frame and Ribs
CC	Double Sided Rubber Strip
D	Glass
DD	Rubber Steel
E	Membrane
EE	Aluminium Strip
F	Wooden Box (chamber)
G	Regenerator Rail
H	Regenerator
J	Metal Base of Regenerator Chamber
K	Hinge
M	Sealing Hinge
N	Regenerator Guide Roller

Figure 2: SCHEMATIC OF THE SOLAR MOTOR

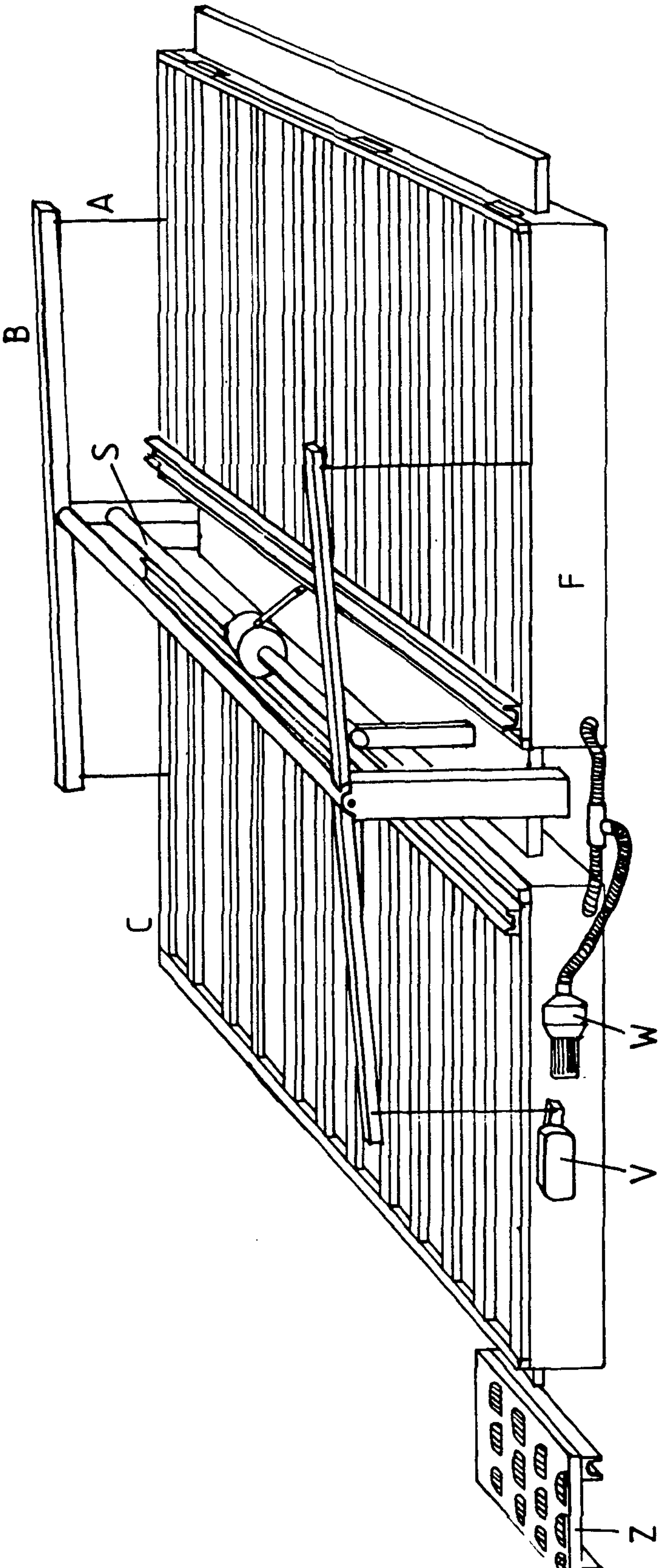

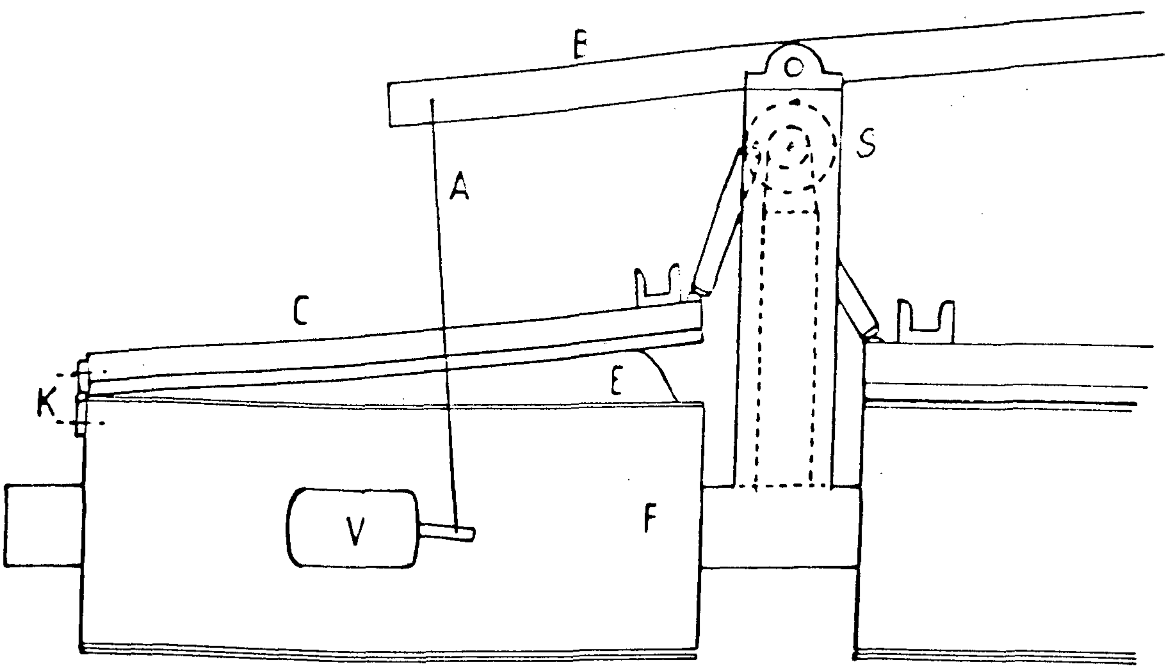

Figure 3

A	Regenerator Cable
B	Drive Aluminium Beam
C	Aluminium Frame and Ribs
E	Membrane in up Position
F	Wooden Box (chamber)
K	Hinge
L	Membrane in Low Position
S	Pump Drive Shaft
V	Electric Boom Drive Motor

REPORT ON THE PREDICTED PERFORMANCE OF A WAGNER SOLAR POWERED LOW TEMPERATURE DIFFERENCE STIRLING TYPE ENGINE

by

C J RALLIS and B M MANGAYA

March 15, 2000

TABLE OF CONTENTS

EXECUTIVE SUMMARY	(iii)
APPENDICES	
A - Solar Energy	1
B - Solar Energy Details	9
C - Solar Radiation Analysis	23
D - Overall Loss Coefficient	30
E - Collector Heat Capacity	49
SOLAR ENGINEERING CLOSING SUMMARY	54
F - Thermodynamic Cycle Analysis	57

EXECUTIVE SUMMARY

This report is made up of two parts. The first, appropriately named Solar Engineering [see pp 54 to 56], deals with the transient energy input to the system and the projected losses by re-radiation, convection and conduction [Appendixes A to E]. This is used to delineate the operating domain throughout the day for specified values of engine and ambient parameters [see figs D7 to D15 pp 42 to 46]. Thus, for example, it is found that there is an optimum value for the clearance between the lower surface of the regenerator/displacer and the bottom plate of the engine. Also, paradoxically, it is shown that the power output of the engine is improved with lower temperature differences between the top and bottom regenerator surfaces. What still requires to be done is to:

- Establish the effect of regenerator thickness and travel on the pressure excursions of the working fluid in the engine.
- find optimum values of the various volumes for given pressure ratios.
- Determine the values of the temperature difference between the top and bottom surfaces of the regenerator for which the engine can operate given the solar radiation available in Cape Town [or anywhere else] during each day over the whole year.
- Check the effect of the thermal inertia of the engine on its heating-up time.
- Select materials, in terms of their solar properties which will yield the required temperature difference between the hot and cold spaces.

The second part of the report (Appendix F) is a first-order, time-independent thermodynamic model for predicting pressure/volume diagrams for the working fluid. This is used to provide information on the effects of various engine parameters. These include clearance space volumes, regenerator/displacer stroke length, and initial cycle pressure. Although admittedly simplistic this model provides useful comparative information. What remains to be explored are the effects of working fluid leakage; structural flexibility; thickness of the regenerator/displacer matrix; regenerator effectiveness; temperature gradients in both the hot and cold spaces; mechanical losses; and the like.

The results obtained with the present model show that of all cases analyzed in this report the present engine yields the lowest power output.

Because of the assumptions made the present model over-predicts the performance of the engine. What requires to be done therefor is to develop a more realistic time dependent second-order model. This should address and try to eliminate as many of the assumptions made in the present model as possible. In particular the dynamics of the displacer and hinged cover must be taken into account.

APPENDIX A

SOLAR ENERGY

A.1 BASIC FLAT-PLATE ENERGY BALANCE EQUATION

Energy balance on the whole collector can be written as [1]:

$$A_c\{[HR(\tau\alpha)]_b + [HR(\tau\alpha)]_d\} = \dot{Q}_U + \dot{Q}_L + \dot{Q}_S \qquad (1)$$

where

H = rate of incidence of beam or diffuse radiation on a unit area of surface of any orientation

R = factor to convert beam or diffuse radiation, to that on the plane of the collector

$(\tau\alpha)$ = transmittance-absorptance product of cover system for beam or diffuse radiation

A_C = collector regenerator area

$\dot{Q}_U$ = rate of useful heat transfer to a working fluid in the solar exchanger

$\dot{Q}_L$ = rate of energy losses from the collector to the surroundings by re - radiation, convection, through supports for the absorber surface. The losses due to reflection from the cover are included in the $(\tau\alpha)$ term above

$\dot{Q}_S$ = rate of energy storage in the collector

b : beam ; d: diffuse

A.2 COLLECTOR OVERALL HEAT TRANSFER COEFFICIENT

Loss coefficient for the top and bottom surfaces is the result of convection, radiation and conduction between parallel plates. The energy transfer between the plate and the cover is equal to the energy lost to the surroundings.

The loss through the top per unit area is:

$$\dot{q}_{loss,top} = h_{reg-c}\left(T_{reg,t} - T_{cover}\right) + \frac{\sigma\left(T^4_{reg,t} - T^4_{cover}\right)}{\dfrac{1}{\varepsilon_{reg,t}} + \dfrac{1}{\varepsilon_{cover}} - 1} \qquad (2)$$

where h_{reg-c} is the heat transfer coefficient between two parallel plates.

If the radiation term is linearized, the heat loss becomes

$$\dot{q}_{loss,top} = \left(h_{reg-C} + h_{r,t}\right)\left(T_{reg,t} - T_{cover}\right) \qquad (3)$$

where

$$h_{r,t} = \frac{\sigma\left(T_{reg,t} + T_{cover}\right)\left(T^2_{reg,t} + T^2_{cover}\right)}{\dfrac{1}{\varepsilon_{reg,t}} + \dfrac{1}{\varepsilon_{cover}} - 1}$$

and

$$R_t = \frac{1}{h_{reg-C} + h_{r,t}} \qquad (4)$$

The resistance from the cover to the surroundings has the same form as equation (4) but the convection heat transfer coefficient is for wind blowing over the collector. The heat loss from flat plates exposed to outside winds are found from a dimensional expression given by McAdams which related the heat transfer coefficient in W/m^2 K to the wind speed in m/s

$$h_{wind} = 5.7 + 3.8V \qquad (5)$$

With reference to the air temperature, the radiation conductance can be written as:

$$h_{c-s} = \varepsilon_{cover}\sigma\left(T_{cover} + T_{sky}\right)\left(T^2_{cover} + T^2_{sky}\right)\frac{\left(T_{cover} - T_{sky}\right)}{\left(T_{cover} - T_a\right)} \qquad (6)$$

$$T_{sky} = 0.0552\ T_{air}^{1.5} \tag{7}$$

where T_{sky} and T_{air} are both in degrees Kelvin. Other relations for T_{sky} are available in the literature.

The resistance to the surroundings is then given by:

$$R_C = \frac{1}{h_{wind} + h_{c-s}} \tag{8}$$

The top loss coefficient from the collector regenerator to the ambient is

$$U_t = \frac{1}{R_t + R_C} = \left(\frac{1}{h_{reg-C} + h_{r,t}} + \frac{1}{h_{wind} + h_{C-s}} \right)^{-1} \tag{9}$$

The procedure for solving the top loss coefficient is an iterative process by noting that:

$$\left(h_{reg-C} + h_{r,t}\right)\left(T_{reg,t} - T_{cover}\right) = U_t\left(T_{reg,t} - T_a\right) \tag{10}$$

$$\left(h_{reg-C} + h_{r,t} - U_t\right)T_{reg,t} = \left(h_{reg,C} + h_{r,t}\right)T_{cover} - U_t T_a$$

Similarly for the bottom:

$$\dot{q}_{loss,bottom} = h_{reg-b}\left(T_{reg,b} - T_{bottom}\right) + \frac{\sigma\left(T_{reg,b}^4 - T_{bottom}^4\right)}{\frac{1}{\varepsilon_{reg,b}} + \frac{1}{\varepsilon_{bottom}} - 1} \tag{11}$$

where h_{reg-b} is the heat transfer coefficient between two parallel plates. Again, if the radiation term is linearized

$$\dot{q}_{loss,bottom} = \left(h_{reg,b} + h_{r,b}\right)\left(T_{reg,b} - T_{bottom}\right) \tag{12}$$

where

$$h_{r,b} = \frac{\sigma\left(T_{reg,b} + T_{bottom}\right)\left(T_{reg,b}^2 + T_{bottom}^2\right)}{\dfrac{1}{\varepsilon_{reg,b}} + \dfrac{1}{\varepsilon_{bottom}} - 1} \tag{13}$$

and

$$R_b = \frac{1}{h_{reg-b} + h_{r,b}} \tag{14}$$

Depending on the attachment of the engine, loss to the surroundings, at the bottom, can be by radiation, convection or conduction. If it is by radiation, then:

$$h_{b-a} = \varepsilon_{bottom}\sigma\left(T_{bottom} + T_a\right)\left(T_{bottom}^2 + T_a^2\right) \tag{15}$$

By conduction

$$h_{b-a} = \frac{k}{L} \tag{16}$$

By forced convection to a fluid flowing along the bottom plate [2]:

$$\overline{Nu} = \overline{h}_{ba}.\frac{L}{k} = 0.664\, Re_L^{1/2}\, Pr^{1/3}; \quad Pr \rangle 0.5 \tag{17}$$

Correction should be made to evaluate the heat transfer coefficient to ambient:

$$h_{b-a} = 0.664\, Re^{1/2}\, Pr^{1/3}\, \frac{k}{L} \frac{\left(T_{bottom} - T_{fluid}\right)}{\left(T_{bottom} - T_a\right)}$$

Again, the temperatures are found by iteration.

The bottom loss coefficient from the collector regenerator to the ambient is

$$U_b = \frac{1}{R_b + R_a} = \left(\frac{1}{h_{reg-b} + h_{r,b}} + \frac{1}{h_{b-a}} \right)^{-1} \qquad (18)$$

We can also write:

$$\left(h_{reg.b} + h_{r,b}\right)\left(T_{reg.b} - T_{botom}\right) = U_b\left(T_{reg.b} - T_a\right)$$

The overall loss coefficient, U_L is :

$$U_L = U_t + U_b \qquad [W/m^2 K] \qquad (19)$$

The edge loss is generally neglected, but it is a loss by conduction, through a thin layer of air.

In the case of plastic cover, some infrared radiation passes directly through the cover. The net radiant energy transfer directly between the collector regenerator and the sky is:

$$\dot{q}_{reg-sky} = \tau \varepsilon_{reg,t} \sigma \left(T_{reg,t}^4 - T_{sky}^4\right) \qquad (20)$$

where τ is the transmittance of the cover for radiation from the regenerator. The top loss coefficient then becomes

$$U_t = \tau \varepsilon_{reg,t} 4\sigma \overline{T}^3 \frac{\left(T_{reg,t} - T_{sky}\right)}{\left(T_{reg,t} - T_a\right)} + \left(\frac{1}{h_{reg-C} + h_{r,t}} + \frac{1}{h_{wind} + h_{C-S}} \right)^{-1} \qquad (21)$$

A.3 USEFUL HEAT TRANSFER

If

$$S = [HR(\tau\alpha)]_b + [HR(\tau\alpha)]_d \tag{22}$$

then, the useful heat transfer is

$$\dot{Q}_U = A_C \left[S - U_L\left(T_{reg\,mean} - T_a\right)\right] \tag{23}$$

The useful heat transfer must be transferred to the fluid:

$$\dot{Q}_U = \frac{\left(T_{reg\,mean} - T_f\right)}{R_{reg-f}} . A_{reg-f} \tag{24}$$

where $R_{reg\text{-}f}$ is the heat transfer resistance between the regenerator and the fluid. For both liquid and air systems, the major heat transfer resistance between the regenerator and the fluid is the convection heat transfer coefficient

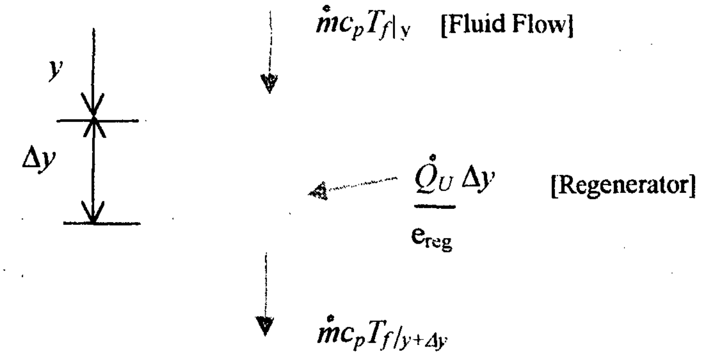

$$\dot{m}c_p T_{f|y} - \dot{m}c_p T_{f|y+\Delta y} + \Delta y \frac{\dot{Q}_U}{e_C} = 0$$

$$\dot{m}c_p \frac{dT_f}{dy} - \frac{A_C}{e_C}\left[S - U_L\left(T_f - T_a\right)\right]F = 0$$

$$\dot{m}c_p \frac{dT_f}{dy} - \frac{A_C}{e_C} SF + \frac{A_C U_L F}{e_C} T_f - \frac{A_C U_L F}{e_C} T_a = 0$$

$$\frac{\dot{m}c_p e_C}{A_C U_L F}\frac{dT_f}{dy} - \frac{S}{U_L} + T_f - T_a = 0$$

$$\frac{T_f - T_a - \frac{S}{U_L}}{T_{f,i} - T_a - \frac{S}{U_L}} = e^{-\left[\frac{U_L A_C F y}{\dot{m}c_f e_C}\right]} \qquad (25)$$

A.4 HEAT CAPACITY EFFECTS

The operation of most solar energy systems is transient. The amount of preheating that will occur in a given collector can be calculated by solving the transient energy balance equations for the various parts of the collector. Even though these equations can be developed to almost any desired degree of accuracy, the driving forces such as solar radiation, wind speed, and ambient temperature are usually known only at hourly intervals.

An energy balance on the regenerator, air and bottom plate yields:

$$(mc)_{reg}\frac{dT_{reg,mean}}{d\tau} = A_C\left[S + U_1\left(T_{cover} - T_{reg,mean}\right)\right] \qquad (26)$$

U_1 is the loss coefficient from the regenerator to the cover. An energy balance on the cover yields:

$$(mc)_{cover}\frac{dT_C}{d\tau} = A_C\left[U_1\left(T_{reg,mean} - T_{cover}\right) + U_2\left(T_a - T_{cover}\right)\right] \qquad (27)$$

U_2 is the loss coefficient from the cover to the ambient air and T_a is the ambient temperature.

If we assume $(T_{cover} - T_a) / (T_{reg,mean} - T_a)$ remains constant, in other words

$$U_2(T_{cover} - T_a) = U_L(T_{reg,mean} - T_a) \tag{28}$$

then

$$\frac{dT_{cover}}{d\tau} = \frac{U_L}{U_2}\frac{dT_{reg,mean}}{d\tau} \tag{29}$$

Combining (26) and (27) and using (29), we obtain the equation for the mean regenerator temperature

$$\left[(mc)_{reg} + \frac{U_L}{U_2}(mc)_{cover}\right]\frac{dT_{reg,mean}}{d\tau} = A_C\left[S - U_L\left(T_{reg,mean} - T_a\right)\right] \tag{30}$$

The term in the square brackets represents an effective heat capacity of the collector. The collector heat capacity includes the glass, regenerator, air, bottom plate and edges.

$$(mc)_e = (mc)_{reg} + \frac{U_L}{U_2}(mc)_{cover} \tag{31}$$

If we assume that S and T_a remain constant for some period, the solution of equation (30) is:

$$\frac{S - U_L\left(T_{reg,mean} - T_a\right)}{S - U_L\left(T_{reg,meaninitial} - T_a\right)} = exp\left(-\frac{A_C U_L \tau}{(mc)_e}\right) \tag{32}$$

The regenerator mean temperature $T_{reg,mean}$ can be evaluated at the end of each time period by knowing S, U_L, T_a and the regenerator mean temperature at the beginning of the time period.

APPENDIX B

SOLAR ENERGY DETAILS

B.1 DIRECTION OF BEAM RADIATION

ϕ : latitude

δ : declination

s : angle between the horizontal and the plane

γ : surface azimuth angle (zero point being due south, east positive and west positive)

ω : hour angle, solar noon being zero, and each hour equaling 15° of longitude with mornings positive and afternoons negative ($\omega = +15$ for 11:00, and $\omega = -37.5$ for 14:30)

θ_z : zenith angle, the angle between the beam from sun and the vertical

α : solar altitude, the angle between the beam from sun and the horizontal, equal to $(90^o-\theta_z)$

The declination, δ, can be found from the approximation equation of Cooper (1969)

$$\delta = 23.45 \sin\left[360 \frac{284+n}{365}\right] \tag{33}$$

where n is the day of the year

$$\begin{aligned}\cos\theta &= \sin\delta \sin\phi \cos s - \sin\delta \cos\phi \sin s \cos\gamma + \cos\delta \cos\phi \cos s \cos\omega \\ &\quad + \cos\delta \sin\phi \sin s \cos\gamma \cos\omega + \cos\delta \sin s \sin\gamma \sin\omega\end{aligned} \tag{34}$$

Useful relationships for the angle of incidence on surfaces sloped to the north or south can be derived from the fact that surfaces with slope s to the north or south have the same angular relationship to beam radiation as a horizontal surface at an artificial latitude of (ϕ - s):

$$\cos\theta_T = \cos(\phi - s)\cos\delta\cos\omega + \sin(\phi - s)\sin\delta \qquad (35)$$

The angle of incidence (i.e., the zenith angle of the sun) is

$$\cos\theta_z = \sin\delta\sin\phi + \cos\delta\cos\phi\cos\omega \qquad (36)$$

This equation can be solved for the sunrise hour angle, ω_S, when $\theta_z = 90°$

$$\cos\omega_B = -\frac{\sin\phi\sin\delta}{\cos\phi\cos\delta} = -\tan\phi\tan\delta \qquad (37)$$

It also follows that the day length is given by

$$T_d = \frac{2}{15}\cos^{-1}(-\tan\phi\tan\delta) \qquad (38)$$

B.2 ESTIMATION OF AVERAGE SOLAR RADIATION

Radiation data are the best source of information. Lacking these, it is possible to use empirical relationships to estimate radiation from hours of sunshine or percent possible sunshine, or cloudiness. A third alternative is estimation for a particular location by use of data from other locations of similar latitude, topography and climate.

The original Angstrom-type regression equation related mean radiation to clear day radiation (at the location in question) and mean fraction of possible sunshine hours:

$$H_{av} = H'_o\left(a' + b'\frac{n}{N}\right) \qquad (39)$$

where

H_{av}	: average horizontal radiation for the period in question
H'_o	: clear day horizontal radiation for the same period
n	: average daily hours of bright sunshine for same period
N	: maximum daily hours of bright sunshine for same period; day length
a',b'	: constants

A basic difficulty lies in the ambiguity of the terms H'_o and n / N. The latter is an instrument problem while the former stems from lack of definition of what constitutes a clear day. Page (1964) and others have modified the method to base it on extraterrestrial radiation on a horizontal surface

$$H_{av} = H_o\left(a + b\frac{n}{N}\right) \qquad (40)$$

where

H_o is the radiation outside of the atmosphere for the same location, averaged over the time period in question and a and b are modified constants depending on location

Löf et al (1966 a) developed sets of constant a and b for various locations and climate types; these are given in Table 1. Values of N can be determined from equation (38)

H_o can be calculated by

$$H_o = \frac{24}{\pi} I_{sc}\left(\left[1 + 0.033\cos\left(\frac{360n}{365}\right)\right]\left[\cos\phi\cos\delta\sin\omega_s + \frac{2\pi w_s}{360}\sin\phi\sin\delta\right]\right) \qquad (41)$$

where

I_{sc} : solar constant, per hour [4871 kJ/m^2 hour]

n : day of the year

ω_s : sunrise hour angle

The declination can be obtained from equation (33) and the sunrise hour angle from equation (37).

TABLE 1: Climatic constants for use in equation (40)

			Sunshine Hours in Percentage of Possible			
Location	**Climate***	**Veg.**	**Range**	**Avg.**	***a***	***b***
Albuquerque, N. M.	BS - BW	E	68-85	78	0.41	0.37
Atlanta, Ga	Cf	M	45-71	59	0.38	0.26
Blue Hill, Mass.	Df	D	42-60	52	0.22	0.50
Brownsville, Tex.	BS	GDsp	47-80	62	0.35	0.31
Buenos Aires, Arg.	Cf	G	47-68	59	0.26	0.50
Charleston, S.C.	Cf	E	60-75	67	0.48	0.09
Darien, Manchuria	Dw	D	55-81	67	0.36	0.23
El Paso, Tex.	BW	Dsi	78-88	84	0.54	0.20
Ely, Nevada	BW	Bzi	61-89	77	0.54	0.18
Hamburg, Germany	Cf	D	11-49	36	0.22	0.57
Honolulu, Hawaii	Af	G	57-77	65	0.14	0.73
Madison, Winsc.	Df	M	40-72	58	0.30	0.34
Malange, Angola	Aw-BS	GD	41-84	58	0.34	0.34
Miami, Fla.	Aw	E-GD	56-71	65	0.42	0.22
Nice, France	Cs	SE	49-76	61	0.17	0.63
Poona, India	Am	S	25-49	37	0.30	0.51
(Monsoon Dry)			65-89		0.41	0.34
Stanleyville, Congo	Af	B	34-56	48	0.28	0.39
Tamanrasset, Alger.	BW	Dsp	76-88	83	0.30	0.43

* Climatic classification based on Trewartha's climate map (1954, 1961), where climate types are:

Af	: Tropical forest climate, constantly moist; rainfall all through the year;
Am	: Tropical forest climate, monsoon rain; short dry season, but total rainfall sufficient to support rain forest;
Aw	:Tropical forest climate, dry season in winter;
BS	: Steppe or semiarid climate;
BW	: Desert or arid climate;
Cf	: Mesothermal forest climate; constantly moist; rainfall all through the year;
Cs	: Mesothermal forest climate; dry season in winter
Df	: Microthermal snow forest climate; constantly moist; rainfall all through the year;
Dw	: Microthermal snow forest climate; dry season in winter;
B	: Broadleaf evergreen trees;
Bzi	: Broadleaf evergreen, shrubform, minimum height 3 feet, growth singly or in groups or patches;
D	: Broadleaf deciduous trees;
Dsi	: Broadleaf deciduous, shrubform, minimum height 3 feet, plants sufficiently far apart that they frequently do not touch;
Dsp	: Broadleaf deciduous, shrubform, minimum height 3 feet, growth singly or in groups or patches;
E	: Needleleaf evergreen trees;
G	: Grass and other herbaceous plants;
GD	: Grass and other herbaceous plants; broadleaf deciduous trees;
GDsp	: Grass and other herbaceous plants; broadleaf deciduous, shrubforms, minimum height 3 feet, growth singly or in groups or patches;
M	: Mixed: broadleaf deciduous and needleleaf evergreen trees;
S	: Semideciduous: broadleaf evergreen and broadleaf deciduous trees;
SE	: Semideciduous: broadleaf evergreen and broadleaf deciduous trees; needleleaf evergreen trees.

B.3 ESTIMATION OF HOURLY RADIATION FROM DAILY DATA

For purposes of design and evaluation of solar processes, it is often desired to make hour-by-hour performance calculations for the system. It is often necessary to start with daily data and estimate hourly values from the daily numbers. It must be recognized that this is not an exact process. For example, daily total radiation values in the middle range between clear day and completely cloudy day values can arise from various circumstances, such as intermittent heavy clouds, continuous light clouds, or heavy cloud cover for part of the day. There is no way to determine circumstances from the daily totals. However, the methods presented here work best for clear days, because those are the days that produce most of the output of solar processes.

It is also possible on the basis of an analysis by Liu and Jordan (1960), to estimate the average hourly diffuse radiation from the average daily diffuse radiation. They have shown, for horizontal surfaces at a particular station, that the ratio of daily diffuse radiation to the daily total radiation for individual days is nearly a unique function of a cloudiness index, that is, the ratio of daily total radiation to extraterrestrial daily insolation, H/H_o.

B.4 RATIO OF BEAM RADIATION ON TILTED SURFACE TO THAT ON HORIZONTAL SURFACE

For purposes of solar process design, it is often necessary to convert data for hourly radiation on a horizontal surface to radiation on a tilted surface. It follows that:

$$H = H_n \cos\theta_z \;;\; H_T = H_n \cos\theta_T$$

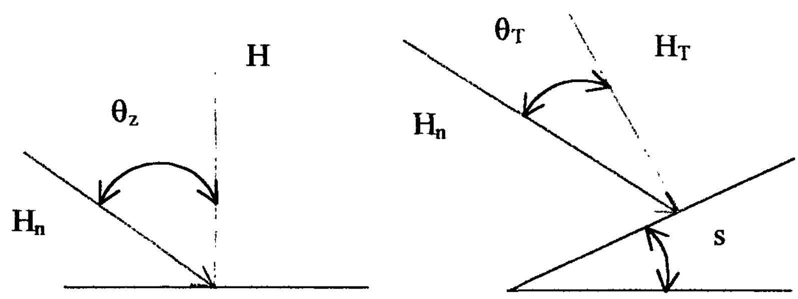

The ratio of radiation on the tilted surface, H_T, to that on the horizontal surface, H, is given in terms of the angle θ_z and θ_T and radiation normal to the beam, H_n, by

$$R_b = \frac{H_T}{H} = \frac{H_n \cos\theta_T}{H_n \cos\theta_z} = \frac{\cos\theta_T}{\cos\theta_z} \tag{42}$$

$$R_b = \frac{\cos\theta_T}{\cos\theta_z} = \frac{\cos(\phi - s)\cos\delta\cos\omega + \sin(\phi - s)\sin\delta}{\cos\phi\cos\delta\cos\omega + \sin\phi\sin\delta} \tag{43}$$

The symbol H is used here for the beam component only.

B.5 RATIO OF TOTAL RADIATION ON A TILTED SURFACE TO THAT ON A HORIZONTAL SURFACE

Flat plate collectors absorb both beam and diffuse components of solar radiation. In order to use horizontal total radiation data, it is necessary to derive a value for R for total solar radiation. The angular correction is straightforward for the beam component. The correction for the diffuse component depends on the distribution of diffuse radiation over the sky, which generally is not known. Two limiting cases have been assumed as a basis for angular correction of the diffuse radiation.

First, it can be assumed that most of the diffuse radiation comes from an apparent origin near the sun, that is, the scattering solar radiation is mostly forward scattering. This approximation will be best on clear days. The angular correction factor to be applied to the diffuse component is essentially the same as that for the beam component, and $R = R_b$.

Second, it can be assumed that the diffuse component is uniformly distributed over the sky. This may be a reasonable approximation when, for example, there is a uniform cloud cover or when conditions are very hazy. Then the diffuse radiation on a surface of other than horizontal orientation is dependent only on how much of the sky the surface sees. If it is further assumed that the properties of the ground or other surfaces seen by a tilted surface reflect solar radiation in such a way as to be a source of diffuse solar radiation equivalent to the sky, then the surface will receive the same diffuse radiation no matter what its orientation. Under this assumption, the correction factor to convert for diffuse radiation is always unity. The radiation on a tilted surface, under these conditions, is:

$$H_T = H_b R_b + H_d \qquad (44)$$

where H_b and H_d are the beam and diffuse components of solar radiation on the horizontal surface, and R_b is the beam correction factor or its equivalent. The effective ratio of solar energy on the tilted surface to that on the horizontal surface is then

$$R = \frac{H_T}{H} = \frac{H_b}{H} R_b + \frac{H_d}{H} \qquad (45)$$

An improvement on this model has been derived by Liu and Jordan (1963) by considering the radiation on the tilted surface to be made up of three components: the beam radiation, diffuse solar radiation and solar radiation reflected from the ground which the tilted surfaces sees. A surface tilted at slope s from the horizontal sees a portion of the sky dome given by $(1+\cos s)/2$; if the diffuse solar radiation is uniformly distributed over the sky dome, this is also the conversion factor for diffuse radiation. The tilted surface also sees ground, or other surroundings and if those surroundings have a diffuse reflectance of ρ for solar radiation, the reflected radiation from the surrounding on the surface from total solar radiation is $(H_b +$

H_d)(1- cos s)ρ /2. Combining the three terms, the total solar radiation on the tilted surface at any time is

$$H_T = H_b R_b + H_d \frac{1+\cos s}{2} + (H_b + H_d)\frac{(1-\cos s)\rho}{2} \qquad (46)$$

and by definition of R:

$$R = \frac{H_b}{H} R_b + \frac{H_d}{H}\frac{1+\cos s}{2} + \frac{(1-\cos s)\rho}{2} \qquad (47)$$

Liu and Jordan suggest values of ground reflectance of 0.2 when there is no snow and 0.7 when there is a snow cover.

None of these approximations is entirely satisfactory. The argument can be made that a solar collector will deliver the largest fraction of its total energy output during periods of high radiation, and that the first assumption is most nearly true under clear sky conditions.

B.6 TRANSMISSION OF RADIATION THROUGH PARTIALLY TRANSPARENT MEDIA

For opaque surfaces, the sum of absorptance and reflectance must be unity. If the surface is transparent to the incident radiation to any degree, the sum of absorptance, reflectance and transmittance must be unity. This relationship holds for surfaces, or layers of a material of finite thickness. Transmittance, like reflectance and absorptance, is a function of wavelength, angle of incidence of the incoming radiation, the refractive index, n, and the extinction coefficient, K, of the material.

Fresnel has derived a relation for the reflection of nonpolarized radiation on passing from a medium 1 with refractive index n_1 to medium 2 with refractive index n_2

$$\frac{I_r}{I_o} = \rho = \frac{1}{2}\left[\frac{\sin^2(\theta_2 - \theta_1)}{\sin^2(\theta_2 + \theta_1)} + \frac{\tan^2(\theta_2 - \theta_1)}{\tan^2(\theta_2 + \theta_1)}\right] \tag{48}$$

where θ_l and θ_2 are angles of incidence and refraction. The angles θ_l and θ_2 are related to the indices of refraction by Snell's law

$$\frac{n_1}{n_2} = \frac{\sin\theta_2}{\sin\theta_1} \tag{49}$$

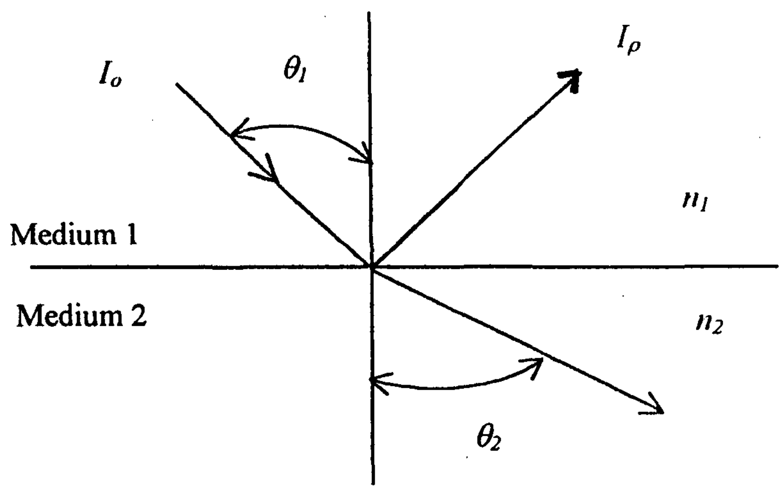

For radiation at normal incidence, both θ_l and θ_2 are 0, and Eqs. (48) and (49) can be combined to yield

$$\rho = \frac{I_r}{I_o} = \left[\frac{(n_1 - n_2)}{(n_1 + n_2)}\right]^2 \tag{50}$$

If one medium is air (i.e., a refractive index of unity) Eq. (50) becomes

$$\rho = \frac{I_r}{I_o} = \left[\frac{(n-1)}{(n+1)}\right]^2 \tag{51}$$

Cover materials used in solar applications require the transmission of radiation through a slab per cover to cause reflection loss. In this situation, the depletion of the beam at the second surface is the same as that at the first, for each component of polarization, assuming the cover interfaces are with air in both sides.

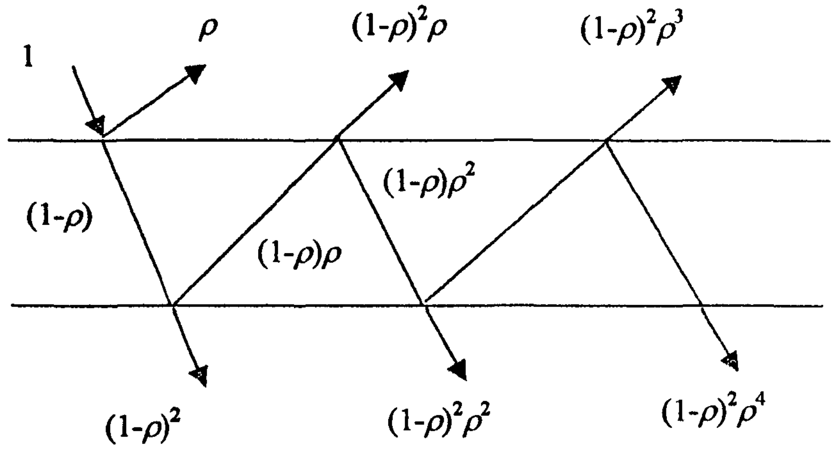

TRANSMISSION THROUGH ONE COVER

The transmittance for a single cover neglecting absorption is:

$$\tau_{r,1} = (1-\rho)^2 \sum_{n=0}^{\infty} \rho^{2n} = \frac{(1-\rho)^2}{(1-\rho^2)} = \frac{1-\rho}{1+\rho} \tag{52}$$

For a system of n covers, all of the same material, a similar analysis yields

$$\tau_{r,n} = \frac{(1-\rho)}{1+(2n-1)\rho} \tag{53}$$

The absorption of radiation in a partially transparent medium is described by Bouger's law, which is based on the assumption that the absorbed radiation is proportional to the local intensity in the medium and the distance the radiation travels in the medium, x:

$$dI = I\,K\,dx \tag{54}$$

where K is the extinction coefficient and is assumed to be a constant in the solar spectrum. Integrating this between limits of 0 and L,

$$\tau_a = \frac{I_L}{I_0} = e^{-KL} \tag{55}$$

For glass, the value of K varies from about 0.04/cm for 'water white' glass to about 0.32/cm for poor (greenish cast of edge) glass. Note that τ_a is the transmittance considering only absorption, and that L is the actual path of the radiation through the medium.

To obtain the transmittance allowing for both reflection and absorption, it is only necessary to multiply the two transmittances together

$$\tau = \tau_r . \tau_a \tag{56}$$

This is a satisfactory relationship provided the product KL is small (i.e., τ_a is not too far from unity). This condition is always met in solar collector at angles of practical interest.

B.7 TRANSMITTANCE-ABSORPTANCE PRODUCT

Of the radiation passing through the cover system and striking the regenerator, some is reflected back to the cover system. However, all this radiation is not lost since some is reflected back to the regenerator.

τ is the transmittance of the cover system at the desired angle as calculated from Eq. (56) and α is the angular absorptance of the regenerator. Of the incident energy, $\tau\alpha$ is absorbed by the regenerator and $(1-\alpha)\tau$ is reflected back to the cover system. The reflection from the regenerator is probably more diffuse than specular so that the fraction $(1-\alpha)\tau$ that strikes the cover plate is diffuse radiation and $(1-\alpha)\tau\rho_d$ is reflected back to the regenerator. The multiple reflection of diffuse radiation continues so that the energy ultimately absorbed is

$$(\tau\alpha) = \tau\alpha\sum_{n=0}^{\infty}\left[(1-\alpha)\rho_d\right]^n = \frac{\tau\alpha}{1-(1-\alpha)\rho_d} \qquad (57)$$

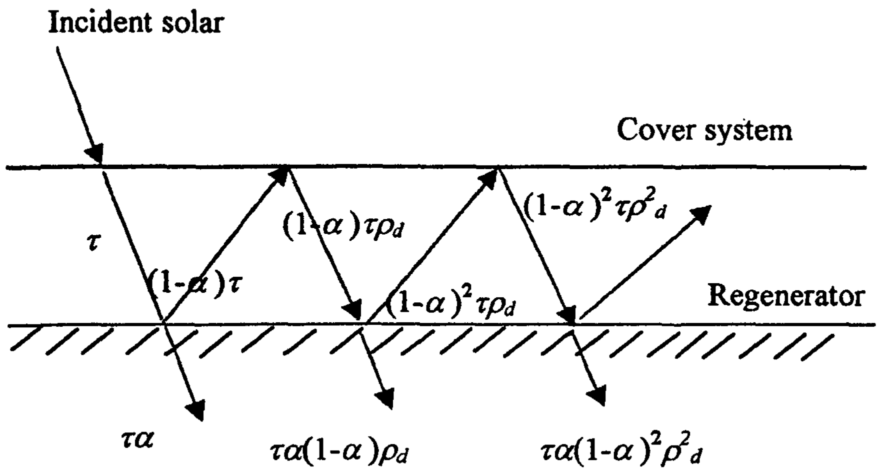

Most transparent media transmit selectively, that is, transmittance is a function of wavelength of the incident radiation. Glass, the material most commonly used as a cover material in solar collectors, may absorb little of the solar energy spectrum if its Fe_2O_3 content is low.

Plastic films may be used as cover materials for solar collectors. In general, they will have transmittances which are more wavelength dependent than glass, and it may be necessary to obtain their transmittance for solar energy by evaluating for monochromatic radiation and then integrating over the solar spectrum.

For most plastics, the transmittance will also be significant in the infrared spectrum at $\lambda < 3\ \mu m$.

B.8 EFFECTS OF SURFACE LAYERS ON TRANSMITTANCE

By the addition of thin films having a refractive index between that of air and the transparent medium, the reflectance of the interfaces can be changed. If a film of low refractive index is deposited at an optical thickness of $\lambda/4$ onto a transparent slab, light reflected from the upper and lower surfaces of the film will have a phase difference of π and will cancel. The reflectance will be decreased and the transmittance will be increased relative to the uncoated material.

Processes have been developed for surface treating glass to reduce its reflectance.

APPENDIX C

SOLAR RADIATION ANALYSES

For solar radiation analyses, equations developed in Appendix B have been used. The following parameters are calculated, given a latitude of 34° for Cape Town:

- declination (Eq. 33)
- sunrise hour (Eq. 37)
- solar radiation outside the atmosphere for the location (Eq. 40)
- day length (Eq. 38)
- average horizontal radiation (Eq. 40)
- diffuse radiation
- transmission of radiation through partially transparent media (eqs. 51,52,55,56 and 57)

The aim of these calculations is to find the terms $HR(\tau\alpha)$ of the basic flat-plate energy balance equation (Eq. 1). It allows also the calculations of the heat capacity effects, the mean regenerator and the cover temperatures, knowing the loss coefficients.

C.1 LATITUDE

$\phi = -34^{\circ}$

C.2 DECLINATION

$n =$ 60 (day of the year; end February)

$$\delta = \mathbf{23.45}\, sin\left[\mathbf{360}\,\frac{\mathbf{284+60}}{\mathbf{365}}\right] = \mathbf{23.45}\, sin(\mathbf{339.288}) = \mathbf{-8.2937}$$

C.3 SUNRISE HOUR

$$\cos \omega_s = -\tan \phi \tan \delta = -\tan(-34^\circ)\tan(-8.2937^\circ) = \mathbf{0.0983244}$$

$$\omega_s = ar\cos(\mathbf{0.0983244}) = \mathbf{84.35} \qquad [6:23 \text{ am}]$$

C.4 SOLAR RADIATION OUTSIDE THE ATMOSPHERE FOR THE LOCATION

$$H_o = \frac{24}{\pi} * 4871 * \left(\left[1 + 0.033\cos\left(\frac{360*60}{365}\right)\right] \left[\begin{array}{l} \cos(-34)\cos(-8.2937)\sin(84.35) \\ + \dfrac{2\pi(84.35)}{360}\sin(-34)\sin(-8.2937) \end{array} \right] \right)$$

$$H_o = \frac{24}{\pi} * 4871 * ([1.01691][0.8250 + 0.11875]) = 35712.4 \text{ kJ/m}^2 \text{ day}$$

$$= \mathbf{1488} \text{ kJ/m}^2 \text{ hour} \qquad \text{(extraterr estrial)}$$

C.5 DAY LENGTH

$$T_d = \frac{2}{15}\cos^{-1}(-\tan \phi \tan \delta) = \frac{2}{15}\cos^{-1}(-\tan(-34)\tan(-8.2937))$$

$$= \frac{2}{15} * 95.64269 = 12.75 \qquad [12:45]$$

C.6 AVERAGE HORIZONTAL RADIATION

$$H_{av} = H_o\left(a + b\frac{n}{N}\right)$$

$$N = \frac{2}{15} cos^{-1}(-tan\phi \, tan\delta) = 12.75$$

$n = 9.8$ (value for Perth, Australia, 32° S)

$a = 0.35$; $b = 0.31$ (value for Brownsville, Texas, 28° S)

$$H_{av} = 1488\left(0.35 + 0.31\frac{9.8}{12.75}\right) = 875.4 \text{ kJ/m}^2 \text{ hour}$$

Approximation of the hourly solar radiation distribution by a cosine function is given as follows:

$$H_{av} * N = H_{av,max} \int_{-6.375}^{6.375} cos \frac{\pi\theta}{N} d\theta$$

where

$H_{av,max}$ is the maximum solar radiation at noon

N is the day length

$$H_{av,max} = \frac{H_{av} * N}{\int_{-6.375}^{6.375} cos \frac{n\theta}{\pi} d\theta} = \frac{875.4 * 12.75}{\left[\frac{12.75}{\pi} sin \frac{\pi\theta}{12.75}\right]_{-6.375}^{6.375}}$$

$$= \frac{11161.35}{\frac{12.75}{\pi} * 2} = 1375 \text{ kJ/m}^2 \text{ hour} = 381.94 \text{ W/m}^2$$

The solar radiation distribution hour by hour for a day (in end February; n = 60) is as follows:

$$6 - 7: H_{av} = 1375 \int_{-6}^{-5} cos \frac{n\theta}{12.75} d\theta = 1375 \left[\frac{12.75}{\pi} sin \frac{\pi\theta}{12.75}\right]_{-6}^{-5}$$

$$H_{av} = 1375 * \frac{12.75}{\pi} * \left[\sin\frac{180 * (-5)}{12.75} - \sin\frac{180 * (-6)}{12.75} \right]$$

$$= 1375 * \frac{12.75}{\pi} * [-0.94315 + 0.99573] = 293.41 \text{ kJ/m}^2 \text{ hour}$$

$$= 81.5 \text{ W/m}^2$$

$$7-8: \quad H_{av} = 1375 * \frac{12.75}{\pi} \left[\sin\frac{180 * (-4)}{12.75} - \sin\frac{180 * (-5)}{12.75} \right]$$

$$= 1375 * \frac{12.75}{\pi} [-0.83360 + 0.94315] = 611.34 \text{ kJ/m}^2 \text{ hour}$$

$$= 169.82 \text{ W/m}^2$$

$$8-9: \quad H_{av} = 1375 * \frac{12.75}{\pi} \left[\sin\frac{180 * (-3)}{12.75} - \sin\frac{180 * (-4)}{12.75} \right]$$

$$= 1375 * \frac{12.75}{\pi} [-0.67369 + 0.83360] = 892.33 \text{ kJ/m}^2 \text{ hour} = 247.87 \text{ W/m}^2$$

$$9-10: \quad H_{av} = 1375 * \frac{12.75}{\pi} \left[\sin\frac{180 * (-2)}{12.75} - \sin\frac{180 * (-3)}{12.75} \right]$$

$$= 1375 * \frac{12.75}{\pi} [-0.47309 + 0.67369] = 1119.43 \text{ kJ/m}^2 \text{ hour}$$

$$= 310.95 \text{ W/m}^2$$

$$10-11: \quad H_{av} = 1375 * \frac{12.75}{\pi} \left[\sin\frac{180 * (-1)}{12.75} - \sin\frac{180 * (-2)}{12.75} \right]$$

$$= 1375 * \frac{12.75}{\pi} [-0.24391 + 0.47309] = 1278.91 \text{ kJ/m}^2 \text{ hour} = 355.25 \text{ W/m}^2$$

$$11-12: \quad H_{av} = 1375 * \frac{12.75}{\pi} [\sin 0 + 0.24391]$$

$$= 1361.13 \text{ kJ/m}^2 \text{ hour} = 378.09 \text{ W/m}^2$$

$$12-13:\ H_{av} = 1375 * \frac{12.75}{\pi}\left[\sin\frac{180}{12.75}\right]$$

$$= 1361.13 \ \text{kJ/m}^2 \text{ hour} = 378.09 \ \text{W/m}^2$$

$$13-14:\ H_{av} = 1375 * \frac{12.75}{\pi}\left[\sin\frac{180*2}{12.75} - \sin\frac{180*1}{12.75}\right]$$

$$= 1375 * \frac{12.75}{\pi}[0.47309 - 0.24391] = 1278.91 \ \text{kJ/m}^2 \text{ hour} = 355.25 \ \text{W/m}^2$$

$$14-15:\ H_{av} = 1375 * \frac{12.75}{\pi}\left[\sin\frac{180*3}{12.75} - \sin\frac{180*2}{12.75}\right]$$

$$= 1375 * \frac{12.75}{\pi}[0.67370 - 0.47309] = 1119.43 \ \text{kJ/m}^2 \text{ hour} = 310.95 \ \text{W/m}^2$$

$$15-16:\ H_{av} = 1375 * \frac{12.75}{\pi}\left[\sin\frac{180*4}{12.75} - \sin\frac{180*3}{12.75}\right]$$

$$= 1375 * \frac{12.75}{\pi}[0.83360 - 0.67370] = 892.34 \ \text{kJ/m}^2 \text{ hour} = 247.87 \ \text{W/m}^2$$

$$16-17:\ H_{av} = 1375 * \frac{12.75}{\pi}\left[\sin\frac{180*5}{12.75} - \sin\frac{180*4}{12.75}\right]$$

$$= 1375 * \frac{12.75}{\pi}[0.94315 - 0.83360] = 611.34 \ \text{kJ/m}^2 \text{ hour} = 169.82 \ \text{W/m}^2$$

$$17-18:\ H_{av} = 1375 * \frac{12.75}{\pi}\left[\sin\frac{180*6}{12.75} - \sin\frac{180*5}{12.75}\right]$$

$$= 1375 * \frac{12.75}{\pi}[-0.83360 + 0.94315] = 611.34 \ \text{kJ/m}^2 \text{ hour} = 169.82 \ \text{W/m}^2$$

C.7 DIFFUSE RADIATION

$$\frac{H_{av}}{H_o} = \frac{875.4}{1488} = 0.588$$

Thus from Duffie J A and Beckman W A, page 47, figure 3.5.2, the ratio of daily diffuse to total daily radiation is [1]:

$$\frac{H_d}{H_{av}} = 0.333$$

C.8 TRANSMISSION OF RADIATION THROUGH PARTIALLY TRANSPARENT MEDIA

Reflection at interface for a horizontal plan, with $n_1 = 1.526$ (glass) and $n_2 = 1$ (air):

$$\rho = \frac{I_r}{I_o} = \left[\frac{n-1}{n+1}\right]^2 = \left(\frac{1.526-1}{1.526+1}\right)^2 = 0.0434$$

Neglecting absorption, the transmittance for a single cover is:

$$\tau_r = \frac{1-\rho}{1+\rho} = \frac{1-0.0434}{1+0.0434} = 0.917$$

The absorption of radiation is given as follows:

$$\tau_a = e^{-KL} \qquad [L = 0.006 \text{ m}; \ K = 0.04 / cm]$$

$$= e^{-4*0.006} = 0.976$$

The transmittance allowing for both reflection and absorption is:

$$\tau = \tau_r . \tau_a = 0.917 * 0.976 = 0.895$$

For $\alpha = 0.80$ and $\rho_d = (1\text{-}\tau_r) = (1\text{-}0.917) = 0.083$

$$(\tau\alpha) = \frac{\tau\alpha}{1-(1-\alpha)\rho_d} = \frac{0.895 * 0.80}{1-(1-0.80)\ 0.083} = \frac{0.716}{0.9834} = 0.728$$

APPENDIX D

OVERALL LOSS COEFFICIENT

D.1 INTRODUCTION

The performance of the engine is described by an energy balance (equation 1). There is a distribution of the incident solar energy into useful energy and various losses.

The loss coefficient for the top surface is the result of convection and radiation between the regenerator and the cover. From the cover, heat is lost to the ambient by wind blowing over the top and by exchange radiation with the sky (equation 9; Appendix A):

$$U_t = \left(\frac{1}{h_{reg-C} + h_{r,t}} + \frac{1}{h_{wind} + h_{C-S}} \right)^{-1}$$

The energy loss through the bottom is heat flow by radiation and convection from the regenerator to the bottom plate. And from the bottom plate, heat is lost by conduction and convection to the fluid. Thus, the bottom loss coefficient is given by equation 18 (Appendix A);

$$U_b = \left(\frac{1}{h_{reg-b} + h_{r,b}} + \frac{1}{h_{b-a}} \right)^{-1}$$

The overall loss coefficient, U_L, is found by adding together the top and bottom coefficients

$$U_L = U_t + U_b \qquad [\mathrm{W/m^2\ K}]$$

D.2 TOP LOSS COEFFICIENT, U_t

A detailed calculation for finding the top loss coefficient is given as follows:

Assuming

$T_{air} = 20^o = 293$ K

$T_{cover} = 35^o = 308$ K

$\varepsilon_{reg,t} = 0.85$ (paper, teflon, rubber,...)

$\varepsilon_{cover} = \varepsilon_{glass} = 0.87$

Given

$T_{reg,t} = 115^o$ C = 388 K

frequency = 1 Hz; $v = 270$ mm/s

Regenerator area = 1.230*2.550 = 3.1365 m^2

$$Re = \frac{\rho v D_h}{\mu} = \frac{vD_h}{\upsilon} = \frac{0.27 * 2 * 0.150}{21.30 * 10^{-6}} = 3802.8$$

γ_{air} is evaluated at (308+388)/2 = 348 K $\approx$ 360 K

The flow is turbulent; [equation 4.45; Mills - Heat Transfer]

$$Nu_D = \frac{(f/8)(Re_D - 1000)Pr}{1 + 12.7(f/8)^{1/2}(Pr^{2/3} - 1)} \qquad 3000 < Re_D < 10^6$$

$f \approx 0.05$; assumed (Moody Chart)

$$Pr = \frac{c_p \mu}{k} = \frac{1007 * 20.94 * 10^{-6}}{0.0306} = 0.689$$

$$Nu_D = \frac{(0.05/8)[3802.8 - 1000]0.689}{1 + 12.7(0.05/8)^{1/2}\left[(0.689)^{2/3} - 1\right]} = \frac{12.0695575}{0.779207859}$$

$$= 15.48811639$$

$$Nu = \frac{h_C L}{k} \rightarrow h_C = \frac{Nu\ k}{L} = \frac{15.48811639\ * 0.0306}{0.150} = 3.160\ \ \mathrm{W/m^2\ K}$$

$$h_{reg-C} = 3.160\ \ \mathrm{W/m^2\ K}$$

Assuming $v_{wind} = 2$ m/s

$$h_{wind} = 5.7 + (3.8 * 2) = 13.3\ \mathrm{W/m^2\ K}$$

$$T_{sky} = 0.0552(293)^{1.5} = 276.8\ \mathrm{K}$$

$$h_{r,t} = \frac{\sigma\left(T_{reg,t} + T_{cover}\right)\left(T_{reg,t}^2 + T_{cover}^2\right)}{\frac{1}{\varepsilon_{reg,t}} + \frac{1}{\varepsilon_{cover}} - 1} = \frac{5.67 * 10^{-8} * (388 + 308) * \left(388^2 + 308^2\right)}{\frac{1}{0.85} + \frac{1}{0.87} - 1}$$

$$= \frac{5.67 * 10^{-8} * 696 * 245408}{1.325895876} = 7.3045\ \ \mathrm{W/m^2\ K}$$

$$h_{cs} = \varepsilon_{cover}\,\sigma\left(T_{cover} + T_{sky}\right)\left(T_{cover}^2 + T_{sky}^2\right)\frac{\left(T_{cover} - T_{sky}\right)}{\left(T_{cover} - T_a\right)}$$

$$= 0.87 * 5.67 * 10^{-8} * (308 + 276.8)\left(308^2 + 276.8^2\right)\frac{(308 - 276.8)}{(308 - 293)}$$

$$= 0.87 * 5.67 * 10^{-8} * 584.8 * 171482.24 * 2.08 = 10.289\ \ \mathrm{W/m^2\ K}$$

$$U_t = \left(\frac{1}{h_{reg-C} + h_{r,t}} + \frac{1}{h_{wind} + h_{C-S}}\right)^{-1} = \left(\frac{1}{3.160 + 7.3045} + \frac{1}{13.3 + 10.289}\right)^{-1}$$

$$= \left(\frac{1}{10.4645} + \frac{1}{23.589}\right)^{-1} = (0.13795)^{-1} = 7.2488\ \ \mathrm{W/m^2\ K}$$

D.3 BOTTOM LOSS COEFFICIENT, U_b

A detailed calculation for finding the bottom loss coefficient is given as follows:

Assuming

$T_{air} = 20^o$ C = 293 K

$T_{reg,b} = 80^o$ C = 353 K

$\varepsilon_{reg,b} = 0.85$

$\varepsilon_{bottom} = 0.20$ (aluminum weathered alloy 75S-T6; $k \approx 170$ W/m K; $L = 0.005$ m)

Given

$T_{bottom} = 25^o$ C = 298 K; $T_{water} = 20^o$ C = 293 K

Frequency = 1 Hz; v = 270 mm/s

Regenerator area = 1.230*2.550 = 3.1365 m^2

$$Re = \frac{\rho v D_h}{\mu} = \frac{v D_h}{\upsilon} = \frac{0.27 * 2 * 0.150}{18.37 * 10^{-6}} = 4409.4$$

γ_{air} is evaluated at (298+353)/2 = 325.5 ≈ 330 K

The flow is turbulent; [equation 4.45; Mills - Heat Transfer]

$$Nu = \frac{(f/8)(Re_D - 1000)Pr}{1 + 12.7(f/8)^{1/2}(Pr^{2/3} - 1)} \qquad 3000 < Re_D < 10^6$$

$f \approx 0.05$; assumed (Moody Chart)

$$Pr = \frac{c_p \mu}{k} = \frac{1006 * 19.71 * 10^{-6}}{0.0287} = 0.69$$

$$Nu = \frac{(0.05/8)(4409.4 - 1000)0.69}{1 + 12.7(0.05/8)^{1/2}(0.69^{2/3} - 1)} = \frac{14.7030375}{0.779965519} = 18.85$$

$$h_{reg-b} = \frac{Nu\ k}{L} = \frac{18.85 * 0.0287}{0.150} = 3.607 \text{ W/m}^2\text{ K}$$

$$h_{r,b} = \frac{\sigma\left(T_{reg.b} + T_{bottom}\right)\left(T_{reg.b}^{2} + T_{bottom}^{2}\right)}{\frac{1}{\varepsilon_{reg.b}} + \frac{1}{\varepsilon_{bottom}} - 1} = \frac{5.67 * 10^{-8} * (353 + 298)(353^{2} + 298^{2})}{\frac{1}{0.85} + \frac{1}{0.20} - 1}$$

$$= \frac{7.877436632}{5.176470588} = 1.522 \text{ W/m}^{2}\text{ K}$$

Conduction through the bottom plate

$$h_{b.a|1} = \frac{k}{L} = \frac{170}{0.005} = 34000 \text{ W/m}^{2}\text{ K}$$

Forced convection by a fluid along the bottom plate

$$Re_{L} = \frac{vL}{\upsilon} = \frac{0.020 * 2.550}{0.87 * 10^{-6}} = 58620.7 \qquad (Re_{transition} = 10^{5})$$

$$v = 0.020 \text{ m/s; assumed}$$

$$Pr = \frac{c_{p}\mu}{k} = \frac{4178 * 8.67 * 10^{-4}}{0.611} = 5.929$$

$$Nu = 0.664 * (58620.7)^{1/2}(5.929)^{1/3} = 290.974$$

$$h_{b.a|2} = \frac{Nu\, k}{L}\frac{\left(T_{bottom} - T_{fluid}\right)}{\left(T_{bottom} - T_{a}\right)} = \frac{290.974 * 0.611 * (298 - 293)}{2.550 * (298 - 293)} = 69.7 \text{ W/m}^{2}\text{ K}$$

Thus:

$$U_{b} = \left(\frac{1}{h_{reg-b} + h_{r,b}} + \frac{1}{h_{b.a|1}} + \frac{1}{h_{b.a|2}}\right)^{-1}$$

$$U_b = \left(\frac{1}{3.607 + 1.522} + \frac{1}{34000} + \frac{1}{69.7} \right)^{-1} = \left(\frac{1}{5.129} + (2.9412 * 10^{-5}) + 0.0143 \right)^{-1}$$

$$= (0.20935)^{-1} = 4.7768 \text{ W/m}^2\text{K}$$

D.4 OVERALL LOSS COEFFICIENT, U_L

$$U_L = U_t + U_b$$

From the previous calculations

$$U_L = 7.2488 + 4.7768 = 12.0256 \text{ W/m}^2\text{K}$$

The above value of U_L is valid for the following conditions:
$T_{air} = 20^o$ C = 293 K ; $T_{cover} = 35^o$ C = 308 K ; $T_{reg,t} = 115^o$ C = 388 K
$T_{reg,b} = 80^o$ C = 353 K; $T_{bottom} = 25^o$ C = 298 K; $T_{water} = 20^o$ C = 293 K
$\varepsilon_{reg} = 0.85$; $\varepsilon_{cover} = 0.87$; $\varepsilon_{bottom} = 0.20$

A Matlab computer code was written to obtain overall loss coefficient for different conditions as given in the table below

TABLE D.1

Figure	Air Temp. (°C)	Fluid Temp.(°C)	Cover Temp. (°C)	Bottom Temp. (° C)	ΔT reg. (° C)
D 1	15	17	20	20	40
D 2	15	17	30	35	40
D 3	20	25	22	22	50
D 4	20	25	30	35	50
D 5	30	20	35	35	50
D 6	30	20	45	50	50

ΔT reg is the temperature difference between the top and the bottom surfaces of the regenerator. In figures D1 to D6, the loss coefficient U_L is plotted versus the bottom regenerator temperature. The position of the regenerator top surface from the cover is given by L. The maximum loss coefficient occurs for $L = 0.150$ m and the minimum one for $L = 0.050$ m. Compared to $L = 0.050$ m, the loss coefficient increases for $L = 0.025$ m and $L = 0.000$ m.

Regarding the loss coefficient, an optimum regenerator displacement is obtained between $L = 0.100$ m and $L = 0.050$ m.

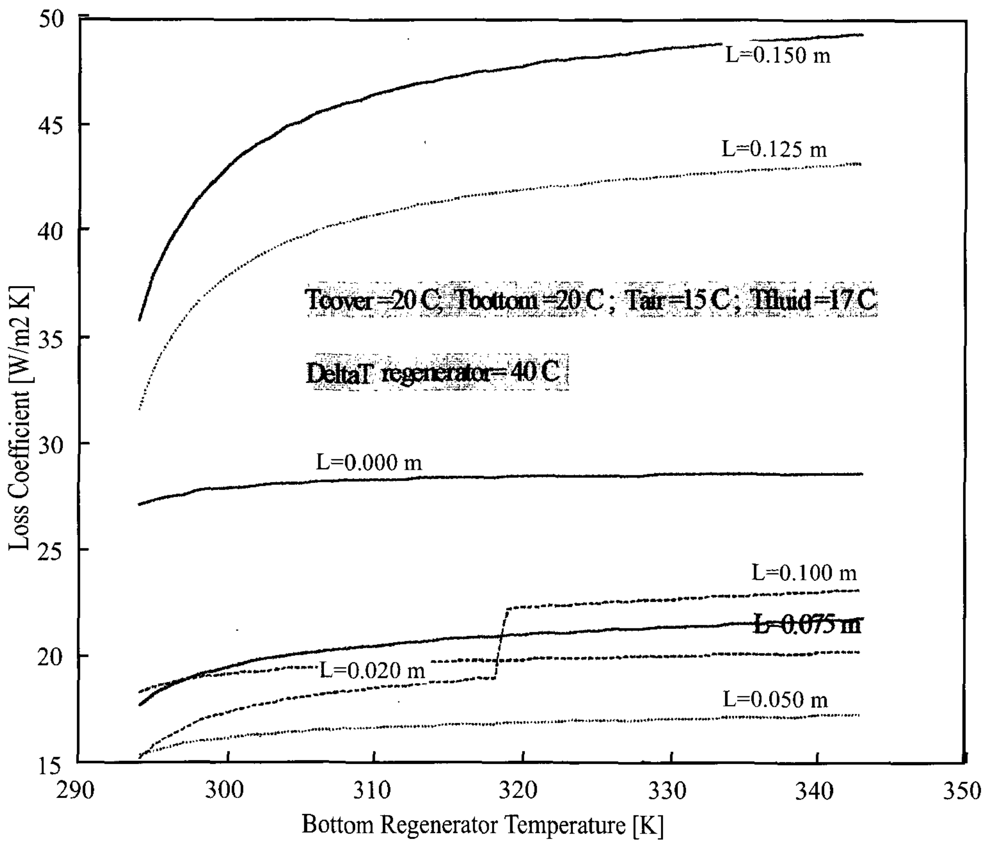

Figure D.1

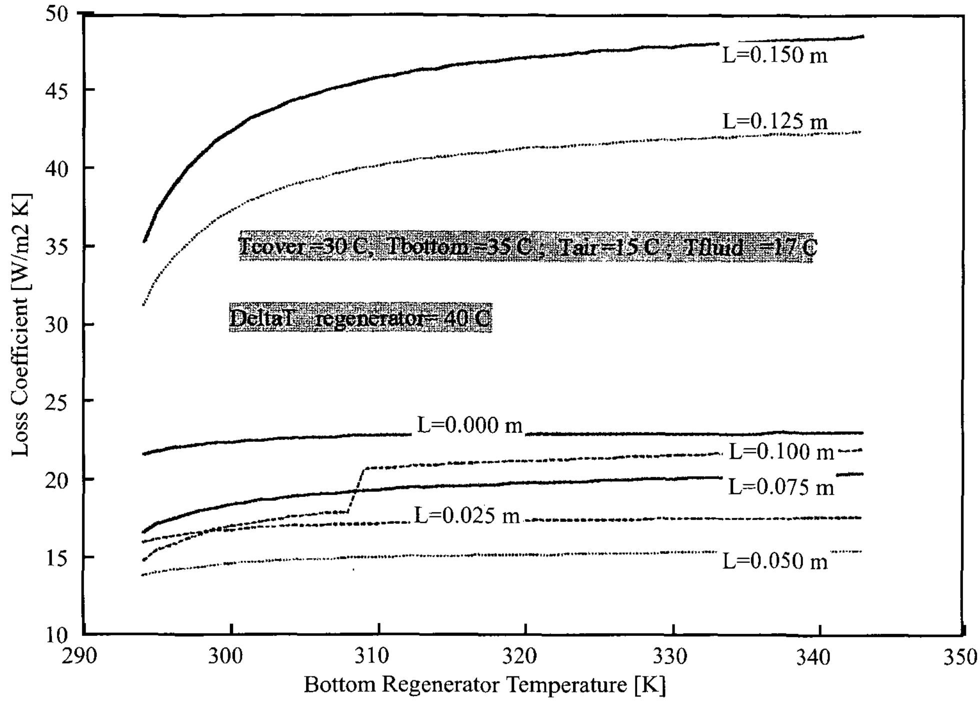

Figure D.2

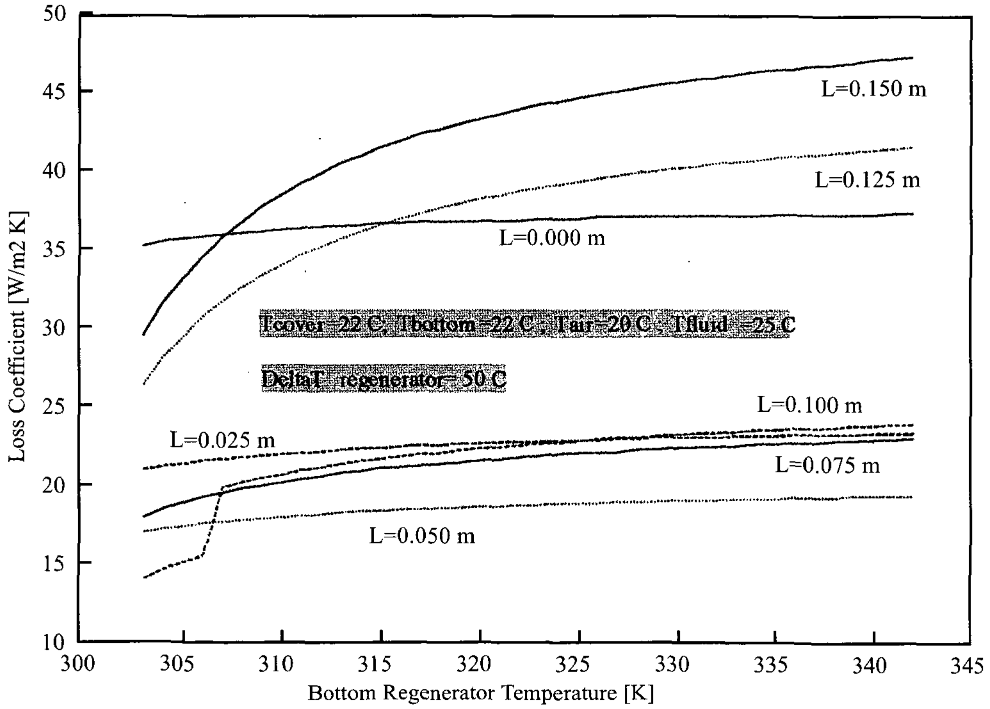

Figure D.3

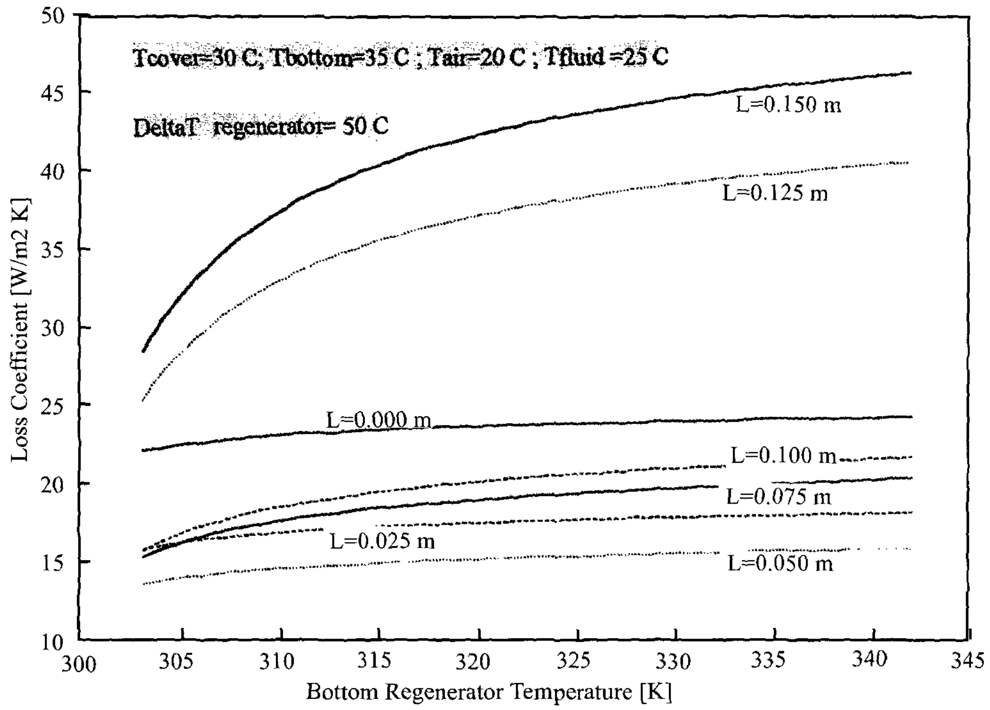

Figure D.4

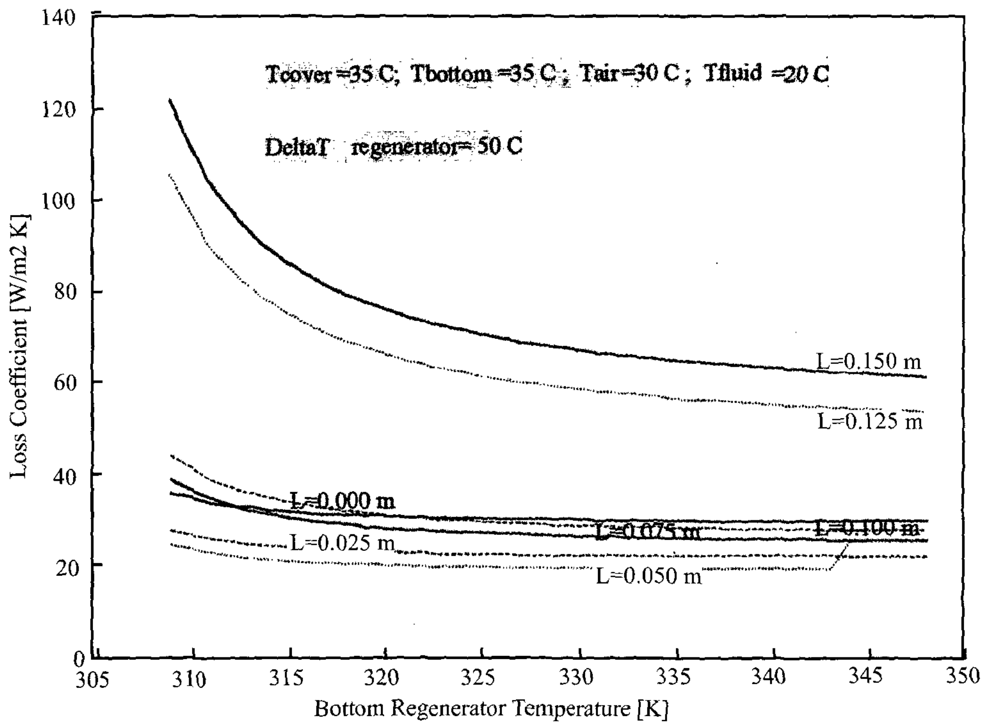

Figure D.5

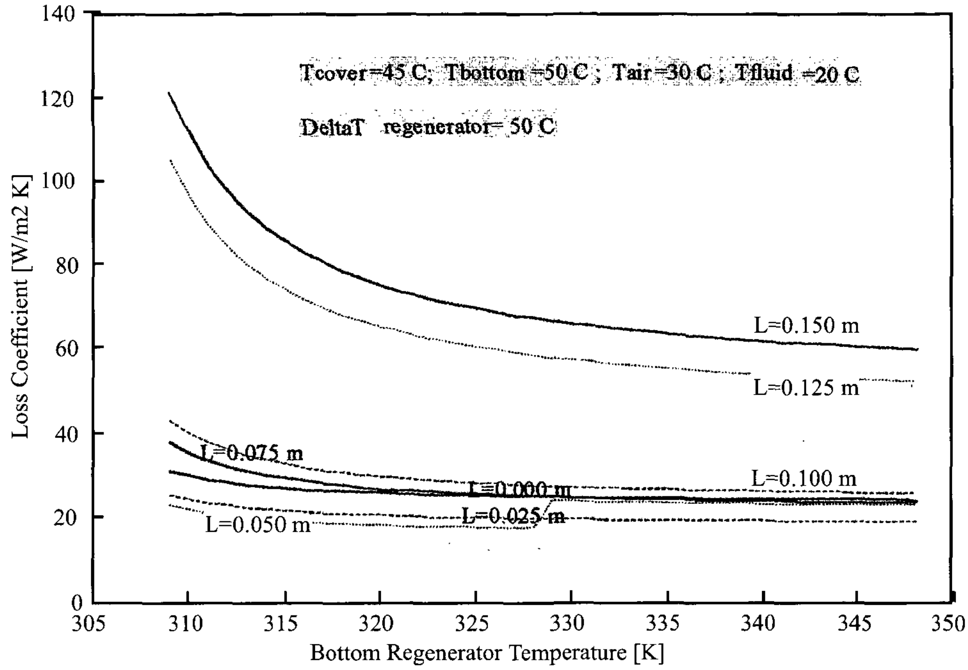

Figure D.6

D.5 OVERALL HEAT LOSS VERSUS SOLAR HEAT GAIN

Referring to equation 1, the overall heat losses can be compared to the incident solar radiation reaching the regenerator to determine the useful heat transfer.

To do so, we have considered solar radiation data from the Weather Bureau for Cape Town. Since the values of global radiation are hourly means, to obtain it in W/m^2, we divide these tabulated values by 3600.

TABLE D.2

HOUR	**GLOBAL RADIATION/ March Weather Bureau (W/m^2)**	**$(\tau\alpha)$ Appendix C.8**	**Solar Heat Gain [W/m^2]**
8-9	458	0.728	333.7
9-10	622.2	0.728	453
10-11	744.4	0.728	542
11-12	805.6	0.728	586.4
12-13	811.1	0.728	590.5

$(\tau\alpha)$ is the transmittance-absorptance product as developed in appendix B.7 and calculated in appendix C.8. The solar heat gain is independent of the bottom regenerator temperature. The overall heat loss is given by the product $U_L(T_{reg,mean} - T_a)$. Considering figure D.1, the following calculations can be made:

(L = 0.075 m; T_{air} = 15° C = 288 K; T_{fluid} = 17° C = 290 K; T_{cover} = 30° C = 303 K; T_{bottom} = 40° C = 313 K)

TABLE D.3

$T_{reg,b}$ Bottom Reg. Temp. [K]	$T_{reg,t}$ Top Reg. Temp. [K]	$T_{reg,mean}$ Mean Reg. Temp. [K]	U_L Loss Coeff. [W/m² K]	($T_{reg,mean}$ - T_a) [K]	U_L ($T_{reg,mean}$ - T_a) Heat Losses [W/m²]
295	315	304	16.5	16	264
300	320	309.9	17.8	21.9	389.8
305	325	314.9	18.4	26.9	494.8
310	330	319.9	18.7	31.9	597
315	335	324.9	19	36.9	701.1
320	340	329.9	19.2	41.9	804.5

where:

$$T_{reg,mean} = \frac{T_{rg,t} - T_{reg,b}}{ln\left(\frac{T_{reg,t}}{T_{reg,b}}\right)}$$

Values of U_L are shown in figure D.16.

The calculation procedure followed in Table D.2 and D.3 is used to plot figures D.7, D.8, D.9, D.10, D.11, D.12, D.13, D.14 and D.15.

For example, in figure D.7, the horizontal lines at the bottom correspond to the values of solar heat gain of Table D.2. The three oblique lines correspond to heat losses for the regenerator positioned respectively at L = 0.075 m, L = 0.025 m and L = 0.050 m. Table D.3 gives value of heat losses at L = 0.075 m for the bottom regenerator temperature between 295 K and 320 K.

The power output per meter square is the difference between the solar heat gain and the heat losses. In figure D.7, at 295 K (= 22° C) as bottom regenerator temperature, the power output is about 300 W/m^2 at 11-13 o'clock.

The parameters used in figures D.7 to D.15 are as follows:

Figure	**Air Temp. (°C)**	**Fluid Temp. (° C)**	**Cover Temp. (° C)**	**Bottom Temp. (° C)**	**ΔT reg. (° C)**
D.7	15	17	30	40	20
D.8	15	17	30	35	20
D.9	15	17	30	35	40
D.10	20	25	30	35	20
D.11	20	25	30	40	20
D.12	20	25	30	35	50
D.13	30	20	45	50	20
D.14	30	20	45	55	20
D.15	30	20	45	50	50

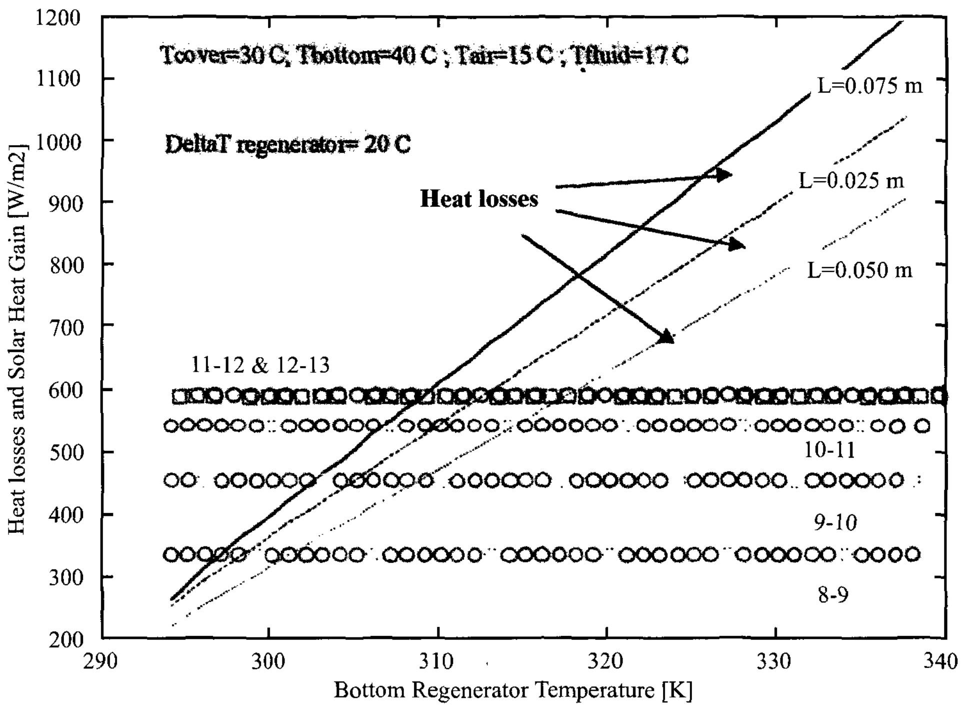

Figure D.7

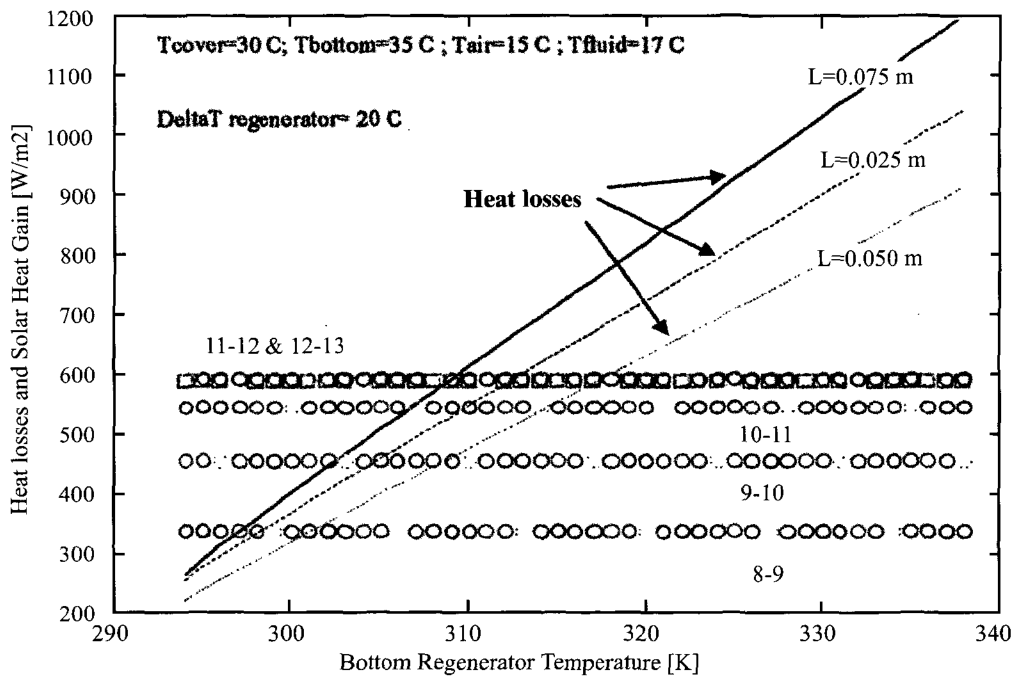

Figure D.8

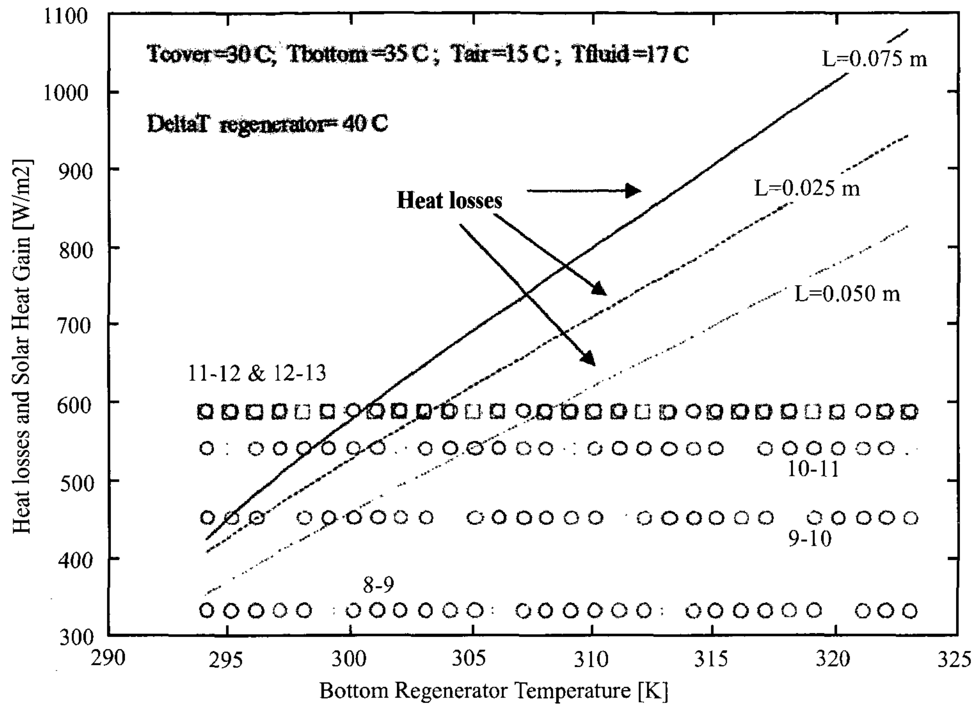

Figure D.9

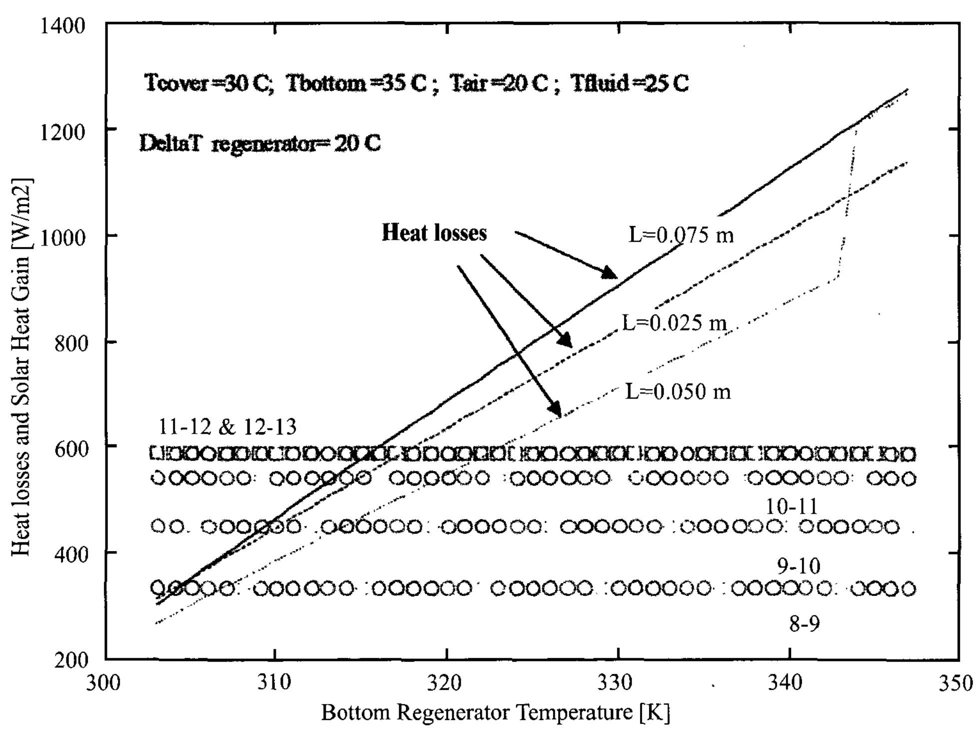

Figure D.10

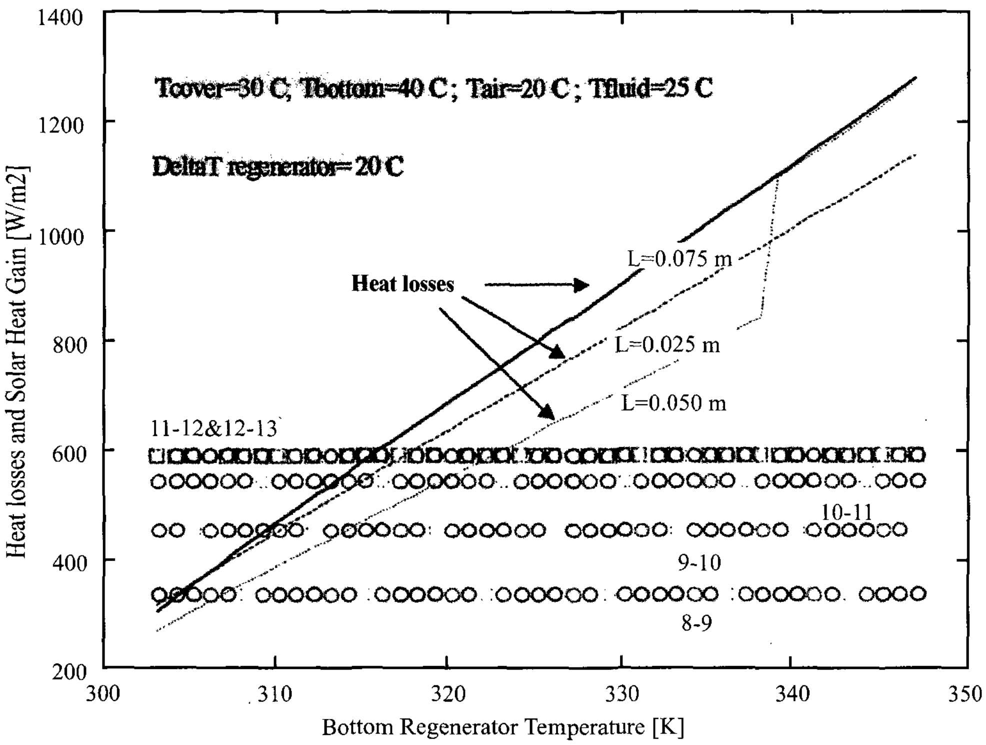

Figure D.11

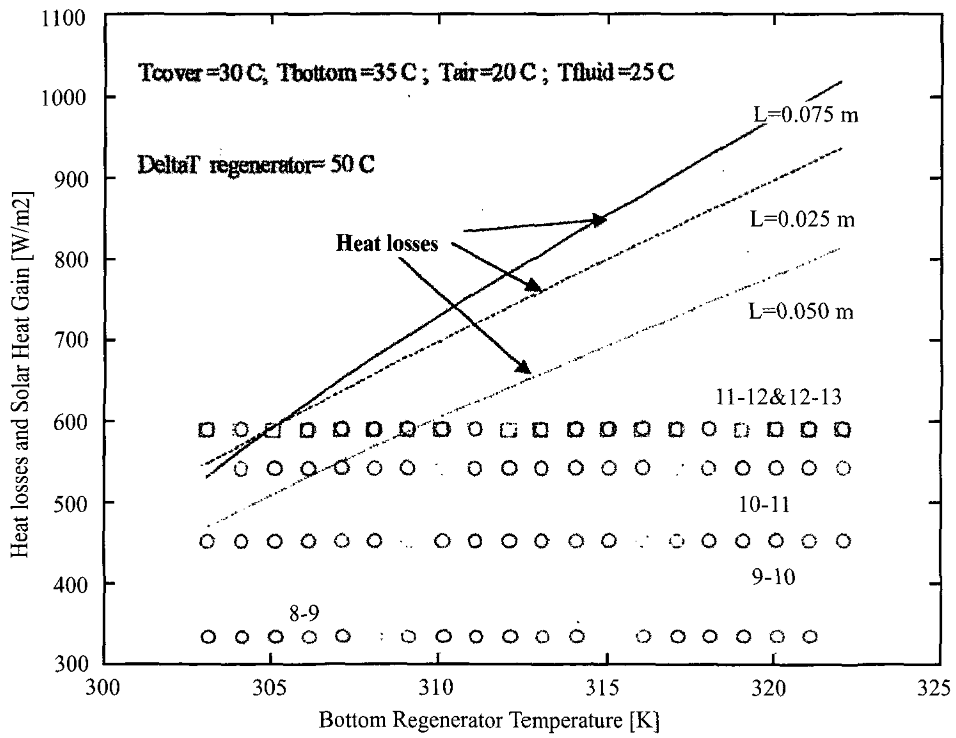

Figure D.12

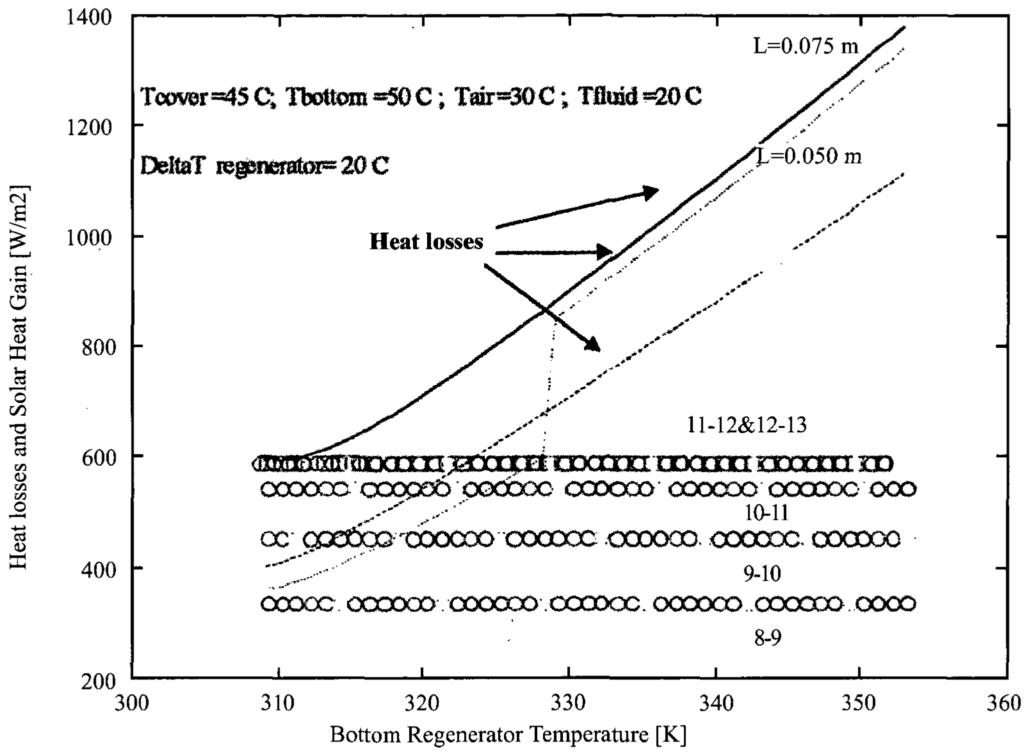

Figure D.13

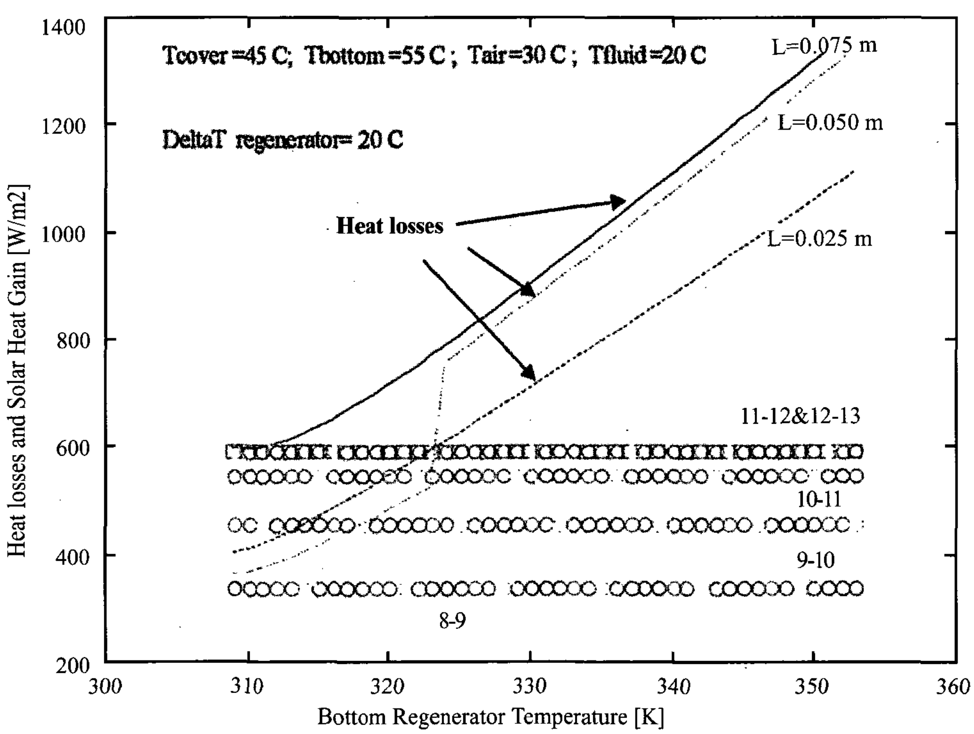

Figure D.14

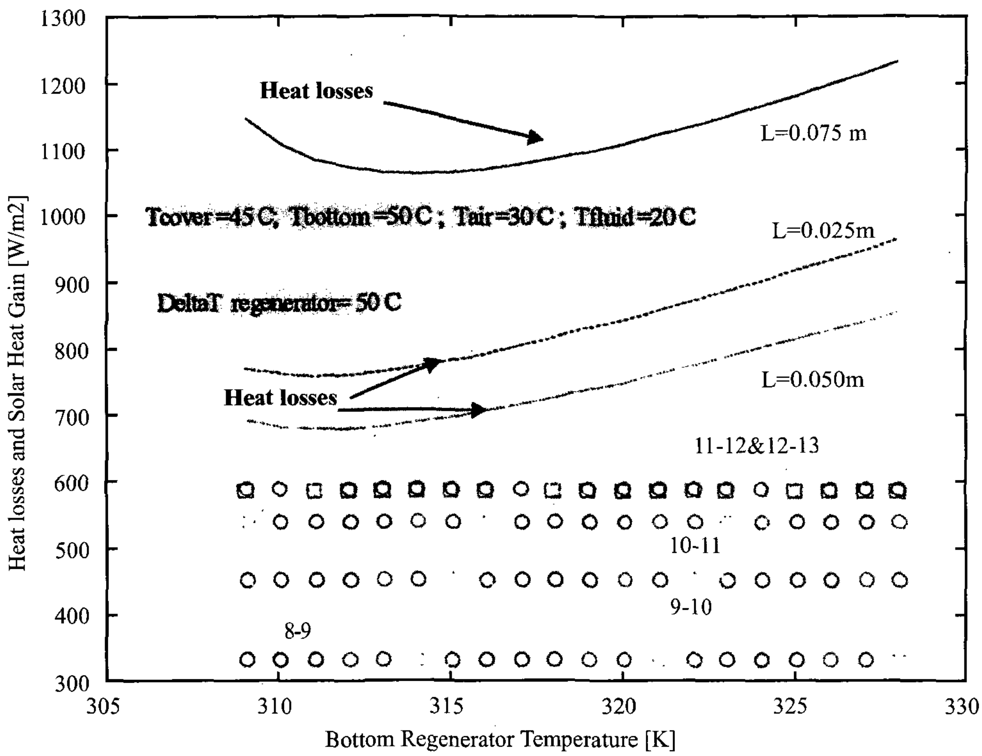

Figure D.15

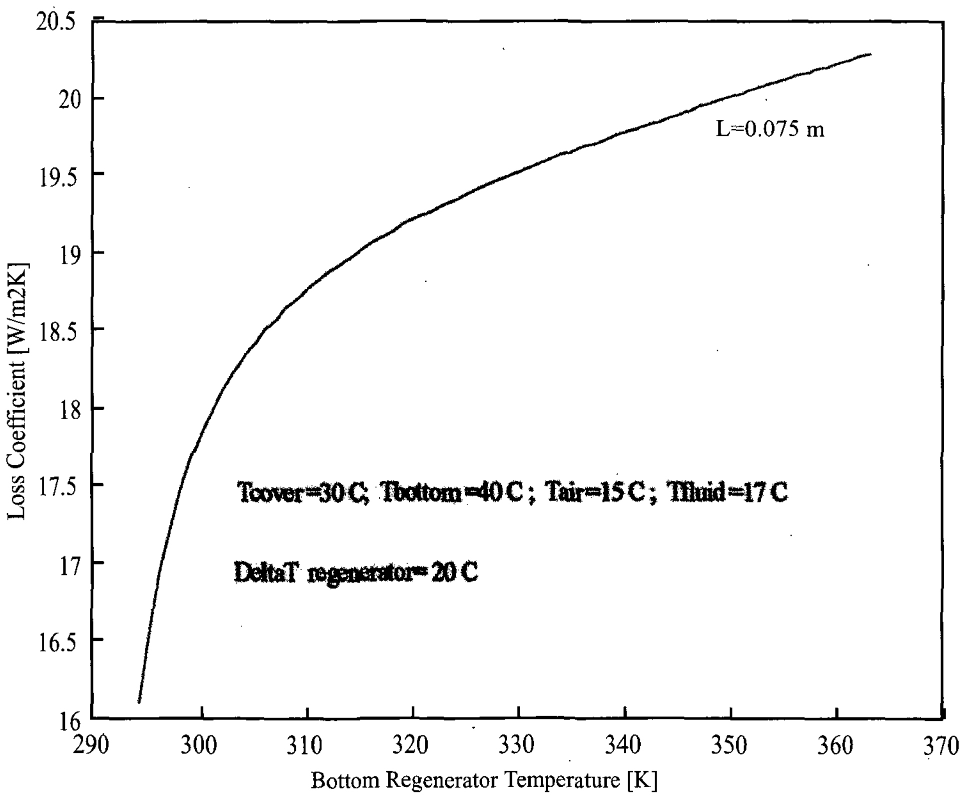

Figure D.16

:T RADIATION						L.A.T. HOUR ENDING							MEGAJOULES/SQ METRE		
	06	07	08	09	10	11	12	13	14	15	16	17	18	19	TOTAL
	.90	1.74	2.21	2.45	2.62	2.79	2.88	2.91	2.92	2.86	2.72	2.51	1.95	.99	32.45
	.30	1.55	2.09	2.39	2.61	2.77	2.89	2.91	2.87	2.82	2.69	2.38	1.70	.35	30.32
	.11	1.21	1.90	2.32	2.57	2.71	2.76	2.79	2.77	2.71	2.46	2.01	1.12	.08	27.50
	.00	.38	1.38	1.86	2.10	2.27	2.36	2.40	2.35	2.25	1.97	1.42	.33	.00	21.08
	.00	.10	.87	1.38	1.70	1.89	1.98	1.99	1.93	1.81	1.50	.92	.09	.00	16.15
	.00	.00	.61	1.23	1.57	1.77	1.80	1.82	1.80	1.62	1.31	.74	.00	.00	14.27
	.00	.01	.79	1.35	1.69	1.86	1.93	1.97	1.92	1.76	1.46	.89	.01	.00	15.64
	.00	.23	1.01	1.48	1.73	1.89	1.92	1.94	1.91	1.81	1.55	1.06	.21	.00	16.74
	.01	.62	1.28	1.63	1.81	1.98	2.09	2.14	2.16	2.08	1.89	1.46	.62	.00	19.76
	.18	1.11	1.62	1.90	2.07	2.24	2.36	2.44	2.47	2.38	2.19	1.87	1.20	.15	24.18
	.61	1.43	1.91	2.17	2.38	2.52	2.65	2.68	2.69	2.64	2.52	2.25	1.73	.72	28.91
	.91	1.65	2.07	2.34	2.50	2.63	2.73	2.82	2.79	2.76	2.64	2.38	1.93	1.14	31.30
.N	.25	.84	1.48	1.87	2.11	2.28	2.36	2.40	2.38	2.29	2.08	1.66	.91	.29	23.19

ISHINE						L.A.T. HOUR ENDING							SUNSHINE HOURS		
	06	07	08	09	10	11	12	13	14	15	16	17	18	19	TOTAL
N	.09	.42	.62	.73	.78	.80	.81	.81	.80	.79	.75	.65	.42	.11	8.59
B	.07	.47	.66	.74	.78	.79	.80	.80	.81	.80	.78	.72	.40	.10	8.72
R	.12	.50	.67	.73	.78	.80	.82	.83	.83	.83	.81	.75	.47	.11	9.05
R	.18	.47	.66	.74	.79	.81	.84	.84	.83	.82	.81	.75	.52	.09	9.14
Y	.27	.44	.65	.75	.79	.82	.84	.85	.86	.84	.83	.74	.52	.14	9.34
JN	.26	.40	.62	.77	.80	.83	.83	.84	.84	.83	.81	.70	.45	.17	9.14
JL	.29	.39	.61	.74	.79	.81	.82	.82	.81	.80	.78	.68	.40	.16	8.90
JG	.24	.40	.60	.73	.77	.80	.81	.81	.81	.81	.79	.66	.44	.09	8.76
EP	.15	.38	.60	.72	.76	.78	.79	.80	.80	.79	.77	.65	.36	.01	8.36
CT	.09	.37	.62	.72	.76	.78	.79	.79	.79	.78	.76	.64	.29	.06	8.22
OV	.06	.33	.59	.68	.72	.74	.75	.75	.74	.74	.71	.60	.25	.06	7.72
EC	.10	.36	.59	.69	.74	.77	.77	.79	.78	.76	.70	.57	.34	.10	8.05
	[illegible]	[illegible]	[illegible]	.73	.77	.79	.81	.81	.81	.80	.78	.68	.40	.10	8.67

·W TOWN HOURLY MEANS

BAL RADIATION L.A.T. HOUR ENDING MEGAJOULES/SQ METRE

	06	07	08	09	10	11	12	13	14	15	16	17	18	19	TOTAL
I	.20	.81	1.53	2.19	2.77	3.24	3.49	3.50	3.31	2.90	2.34	1.65	.88	23	29.02
ı	.07	.58	1.29	1.98	2.59	3.04	3.29	3.30	3.08	2.68	2.11	1.39	.63	.08	26.12
ι	.01	.29	.95	1.65	2.24	2.68	2.90	2.92	2.71	2.30	1.69	.98	.28	.01	21.60
ι	.00	.07	.51	1.11	1.64	2.04	2.26	2.28	2.07	1.69	1.15	.53	.06	.00	15.42
ſ	.00	.01	.22	.69	1.16	1.52	1.71	1.71	1.54	1.20	.73	.23	.01	.00	10.73
ı	.00	.00	.13	.53	.97	1.30	1.46	1.47	1.31	.98	.55	.14	.00	00	8.84
,	.00	.00	.17	.63	1.08	1.42	1.59	1.61	1.44	1.10	.65	.18	.00	.00	9.88
;	.00	.03	.36	.89	1.37	1.73	1.91	1.92	1.75	1.40	.91	.37	.03	.00	12.67
›	.00	.16	.67	1.26	1.77	2.17	2.41	2.44	2.27	1.90	1.36	.72	.15	.00	17.27
ŗ	.04	.43	1.06	1.71	2.24	2.68	2.94	2.98	2.81	2.39	1.83	1.15	.45	.03	22.74
/	.15	.71	1.42	2.09	2.67	3.10	3.35	3.39	3.20	2.81	2.25	1.55	.79	.17	27.65
:	.24	.85	1.57	2.23	2.80	3.23	3.47	3.54	3.32	2.95	2.39	1.70	.95	.28	29.52
AN	.06	.33	.82	1.41	1.94	2.35	2.56	2.59	2.40	2.03	1.50	.88	.35	.07	19.29

FFUSE RADIATION L.A.T. HOUR ENDING MEGAJOULES/SQ METRE

	06	07	08	09	10	11	12	13	14	15	16	17	18	19	TOTAL
N	.09	.28	.43	.56	.65	.69	.71	.69	.64	.58	.51	.41	.29	.11	6.63
B	.04	.22	.38	.51	.60	.64	.63	.63	.59	.54	.46	.36	.22	.05	5.88
R	.01	.12	.30	.43	.50	.56	.58	.59	.54	.48	.40	.29	.12	.00	4.92
R	.00	.04	.20	.36	.48	.55	.58	.57	.54	.46	.35	.21	.04	.00	4.37
Y	.00	.00	.11	.28	.41	.49	.53	.53	.49	.40	.28	.11	.00	.00	3.64
N	.00	.00	.07	.23	.35	.44	.48	.48	.43	.35	.23	.07	.00	.00	3.13
L	.00	.00	.09	.25	.38	.46	.50	.50	.45	.36	.25	.08	.00	.00	3.33
G	.00	.02	.17	.34	.48	.57	.62	.61	.57	.47	.34	.17	.02	.00	4.38
P	.00	.08	.29	.48	.63	.72	.75	.74	.69	.58	.45	.29	.08	.00	5.79
T	.02	.20	.41	.59	.72	.79	.82	.80	.73	.64	.54	.40	.21	.02	6.90
V	.08	.29	.48	.62	.72	.78	.77	.74	.69	.64	.55	.44	.28	.09	7.18
C	.12	.31	.48	.60	.68	.74	.76	.71	.67	.61	.54	.43	.31	.13	7.11
AN	.03	.13	.28	.44	.55	.62	.64	.63	.59	.51	.41	.27	.13	.03	5.27

APPENDIX E

COLLECTOR HEAT CAPACITY EFFECTS

The operation of the engine is transient. The regenerator mean temperature variation during the day can be evaluated using equation 32:

$$\frac{S - U_L\left(T_{reg,mean} - T_a\right)}{S - U_L\left(T_{reg,mean\ initial} - T_a\right)} = exp\left(-\frac{A_C U_L \tau}{(mc)_e}\right) \tag{32}$$

The cover temperature variation during the day is evaluated using equation 29:

$$\frac{dT_{cover}}{d\tau} = \frac{U_L}{U_2}\frac{dT_{reg,mean}}{d\tau} \tag{29}$$

S is evaluated based on data from the Weather Bureau. For hand calculations, *S*is calculated from equations 22 and 40:

$$S = [HR(\tau\alpha)]_b + [HR(\tau\alpha)]_d \tag{22}$$

$$H_{av} = H_o\left(a + b\frac{n}{N}\right) \tag{40}$$

U_L has been calculated in Appendix D for various conditions. For hand calculations, U_L has been taken as obtained in Appendix D.4:

$$U_L = \mathbf{7.2488 + 4.7768 = 12.0256}\ \text{W/m}^2\ \text{K}$$

Since the regenerator is moving, U_L fluctuates between a minimum and a maximum value. Thus, a window can be defined for the mean regenerator temperature variation. Figures E.1, E.2 and E.3 have been obtained in a such way.

The collector heat capacity is calculated as follows (neglecting the edge, the air and the cooling water capacities):

a) Mass of the cover:

$$m_{cover} = \mathbf{2.257 * 1.240 * 0.005 * 220 = 31.065}\ \text{kg}$$

$[c = 800 \text{ J/kg K}; \ \rho = 2220 \text{ kg/m}^3; \ U_{cover} = 23.589 \text{ W/m}^2 \text{ K}]$

Heat capacity of the cover:

$$(mc)_{cover} = 31.065 * 800 = 24852.3 \text{ J/K}$$

b) Mass of the regenerator

$$m_{regenerator} = 2.257 * 1.240 * 0.050 * 45 = 6.297 \text{ kg}$$

$$[c = 1210 \text{ J/kg K}; \ \rho = 45 \text{ kg/m}^3]$$

Heat capacity of the regenerator:

$$(mc)_{regenerator} = 6.297 * 1210 = 7619.4 \text{ J/K}$$

c) Mass of the bottom plate

$$m_{bottom} = 2.257 * 1.240 * 0.005 * 2700 = 37.782 \text{ kg}$$

$$[c = 883 \text{ J/kg K}; \ \rho = 2700 \text{ kg/m}^3]$$

Heat capacity of the bottom plate:

$$(mc)_{bottom} = 37.782 * 883 = 33361.7 \text{ J/K}$$

d) Heat capacity of the collector:

$$(mc)_e = (mc)_{collecxtor} + \frac{U_L}{U_2}(mc)_{cover} = \left[(33361.7 + 7619.4) + \frac{12.0256}{23.589} 24852.3\right] \text{ J/K}$$

$$= (40981.1 + 12669.6) \text{ J/K} = 53650.7 \text{ J/K}$$

e) Time constant

$$\frac{A_C U_L \tau}{(mc)_e} = \frac{(2.257 * 1.240) * 12.0256 * 3600}{53650.7} = 2.258$$

f) Mean regenerator temperature variation:

$$\frac{S - U_L\left(T_{reg,mean} - T_a\right)}{S - U_L\left(T_{reg,mean\ initial} - T_a\right)} = exp\left(-\frac{A_C U_L \tau}{(mc)_e}\right) \tag{32}$$

$$\frac{S - 12.0256\left(T_{reg,mean} - 293\right)}{S - 12.0256\left(T_{reg,mean\ initial} - 293\right)} = e^{-2.258}$$

$$S - 12.0256\left(T_{reg,mean} - 293\right) = \left[S - 12.0256\left(T_{reg,mean\ initial} - 293\right)\right]e^{-2.258}$$

$$T_{reg,mean} = 293 + \frac{S - \left\{\left[S - 12.0256\left(T_{reg,mean\ initial} - 293\right)\right]e^{-2.258}\right\}}{12.0256}$$

g) Cover temperature variation

$$\left(T_{cover} - T_{cover,initial}\right) = \frac{U_L}{U_2}\left(T_{reg,mean} - T_{reg,mean\ initial}\right)$$

From the calculations above, Table E.1 is obtained

TABLE E.1

HOUR	H_{av} [W/m^2]	H_d [W/m^2]	H_b [W/m^2]	R_b	$S=H_{av}(\tau\alpha)$ [W/m^2]	$T_{reg,mean}$ [K]	T_{cover} [K]
6-7	81.5	27.14	54.36	1	63.23	297.7	295.4
7-8	169.82	56.55	113.26	1	131.76	303.3	298.3
8-9	247.87	82.54	165.33	1	192.31	308.4	303.8
9-10	310.95	103.55	207.40	1	241.26	312.6	305.9
10-11	355.25	118.30	236.95	1	252.35	313.8	306.5
11-12	378.09	125.90	252.19	1	293.35	317.0	308.1

TABLE E.1
(Cont.)

HOUR	H_{av} [W/m²]	H_d [W/m²]	H_b [W/m²]	R_b	$S=H_{av}(\tau\alpha)$ [W/m²]	$T_{reg,mean}$ [K]	T_{cover} [K]
12-13	378.09	125.90	252.19	1	293.35	317.3	308.3
13-14	355.25	118.30	236.95	1	252.35	314.3	306.8
14-15	310.95	103.55	207.40	1	241.26	313.2	305.3
15-16	247.87	82.54	165.33	1	192.31	309.4	304.7
16-17	169.82	56.55	113.26	1	131.76	304.5	302.8
17-18	81.5	27.14	54.36	1	63.23	298.9	297.7

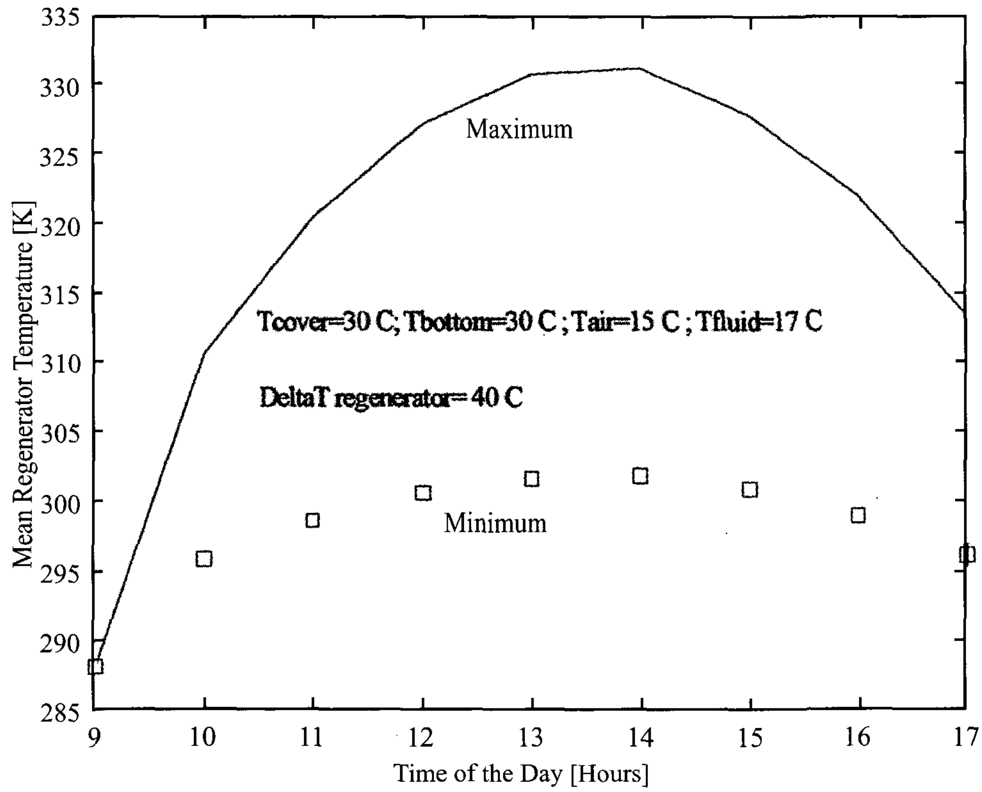

Figure E.1

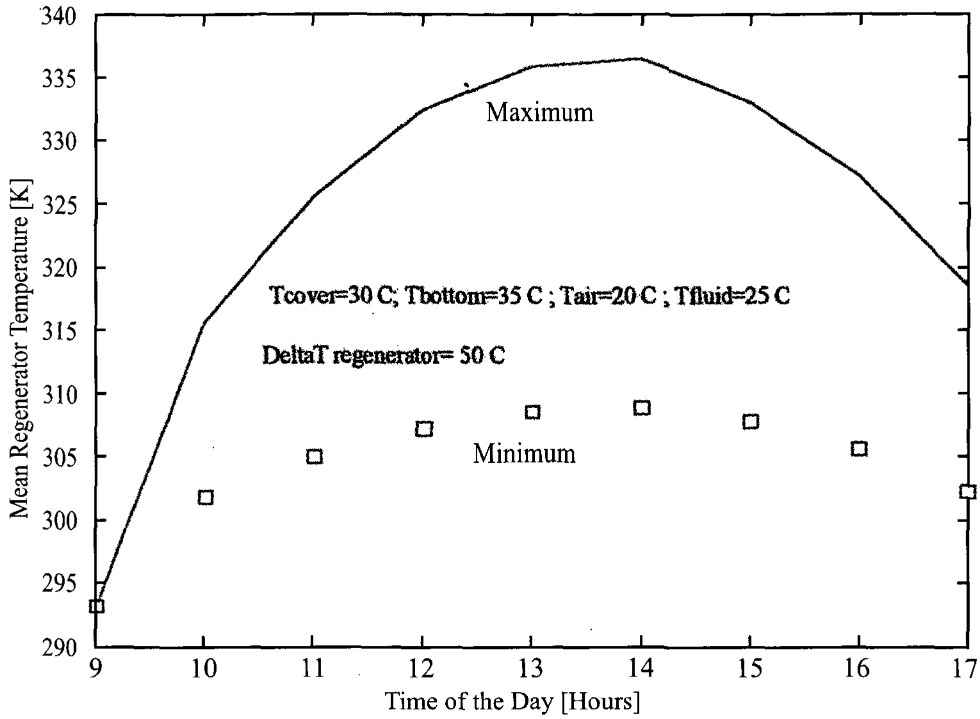

Figure E.2

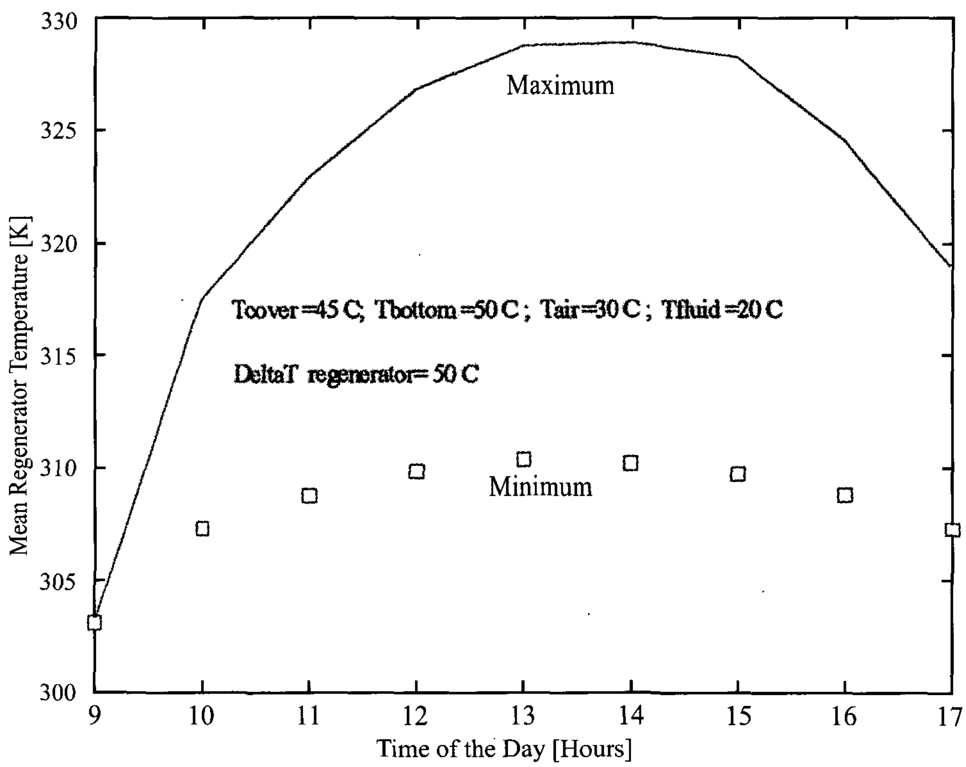

Figure E.3

SOLAR ENGINEERING CLOSING SUMMARY

To predict the operation of the engine, an energy balance has been done for the collector to determine:

- the rate of incident solar radiation reaching the regenerator
- the energy losses by re-radiation, convection and conduction

From this energy balance, the power output can be found, and an optimum range of operating temperatures can be described (figures D.7 to D.15).

The mean regenerator temperature variation, as well as the cover temperature variation during the day are calculated by solving the transient energy balance equations. Since in the present case the losses fluctuate, the temperature variation is set inside a window of minimum and maximum temperature variations (figures E.1 to E.3).

Solar engineering is also used to determine:

- the direction of the beam radiation
- the average solar radiation (Appendix C)
- the ratio of beam radiation on tilted surface to that on horizontal surface
- the transmission of radiation through partially transparent media (Appendix C)
- the transmittance-absorptance product (Appendix C)
- the collector overall heat transfer coefficient (figures D.1 to D.6)

The rate of incident solar radiation is obtained in two ways:

- data from the Weather Bureau
- empirical relationships (Angstrom-type regression equation, Page equation, Löf et al constants,...)

The ratio of radiation on the tilted surface, H_T, to that on the horizontal surface, H, is given in terms of the angles involved.

For the cover, the sum of absorptance, reflectance and transmittance is unity. Of the radiation passing through the cover system and striking the plate, some is reflected back to the cover system. All this radiation is not lost since some is reflected back to the plate. There is multiple reflection of diffuse radiation.

Solar engineering calculations give the following for Cape Town (end February):

- latitude $\phi = -34^o$
- declination $\delta = -8.2937$
- sunrise hour $\omega_s = 84.35$ (6:23 am)
- solar radiation outside the atmosphere $H_o = 1488$ kJ/m^2 hour
- day length $T_d = 12.75$ (12:45)
- average horizontal radiation $H_{av} = 875.4$ kJ/m^2 hour
- diffuse radiation $H_d = 291.5$ kJ/m^2 hour
- transmittance for a single cover (without absorption) $\tau_d = 0.917$
- absorption of radiation $\tau_a = 0.976$
- transmittance $\tau = 0.917*0.976 = 0.895$
- transmittance-absorptance product $(\tau\alpha)$=0.728

In all simulated situations, the overall loss coefficient, for the regenerator moving between $L = 0.100$ m and $L = 0.025$ m, is less than 40 W/m^2 K. Higher values of the overall loss coefficient are obtained when the regenerator moves closer to the bottom plate (L=0.125 m and $L = 0.150$ m).

The overall heat loss is given by the product U_L ($T_{reg,mean}$ - T_a). Its value ranges from 260 W/m^2 to 600 W/m^2 when the bottom regenerator temperature varies between 295 K and 325 K. However, for a high difference between bottom and top regenerator surfaces, the overall heat loss can exceed 600 W/m^2.

The value of 600 W/m^2 corresponds to the solar heat gain at 12-13 o'clock during the month of March. Thus, the operating bottom regenerator temperature should be between 295 K and 325 K for this period to get positive power output.

Apparently, lower temperature difference between top and bottom regenerator surfaces give more useful power output.

Computer simulation shows that at 12-13 o'clock the minimum possible mean regenerator temperature is around 300 K while the maximum possible can be up to 335 K.

REFERENCES

1 - Duffie, J A and Beckman, W A (1974). *Solar Energy Thermal Processes*, John Wiley & Sons, New York.

2 - Mills, A F (1992). *Heat Transfer*, International Student Edition, Richard D Irwin, Boston Massachusetts.

3 - Chauliaguet, C, Baratçabal, P and Batellier, J P (1979). *L'énergie solaire dans le bâtiment,* éditions Eyrolles, Paris.

4 - Duffie, J A and Beckman, W A (1980). *Solar Engineering of Thermal Processes*, John Wiley & Sons, New York.

5 - Kreith, F and Kreider, J F (1978). *Principles of Solar Engineering*, McGraw-Hill Book Company, New York.

APPENDIX F

THERMODYNAMIC CYCLE ANALYSIS

Thermodynamic analysis of the Wagner solar-powered Stirling type engine can be carried out at three levels of complexity: first-order or quasi-static; second-order or lumped parameter; and third-order or dynamic numerical simulation.

For the purpose of this report, it was considered adequate to use a first-order model which could provide information on the effects of various parameters, such as clearance space volumes, initial or minimum cycle pressures, system flexibility, and the like. These results could then be combined with heat transfer predictions, presented in Appendices A to E, to establish operating domains and optimum values.

Unfortunately this thermodynamic analysis, even though it overpredicts the engine performance, shows that in its present form and imposed constraints it yields a relatively low output, even before the effects of working fluid leakage, deflection of the structure and heat transfers are taken into account.

THE WAGNER ENGINE

The Wagner engine is a low ΔT solar-powered Stirling type regenerative prime mover made up of two panels connected together with a phase difference between them of 180 degrees. Each machine is comprised of a box-like structure with a hinged transparent cover (see Fig F.1). Contained within the box is a flat porous regenerator matrix which is moved vertically up and down by a small electric motor.

The working fluid (air) contained above the regenerator is maintained at a high temperature (T_H) while that below it is maintained at a low temperature (T_C). Vertical displacement of the regenerator causes the working fluid to pass through it and in the process transferring thermal energy to or from the porous matrix. Upward motion of the matrix causes energy to be stored within it while downward motion heats up the working fluid. The up and down motion of the hinged cover transfers work to or from the surroundings.

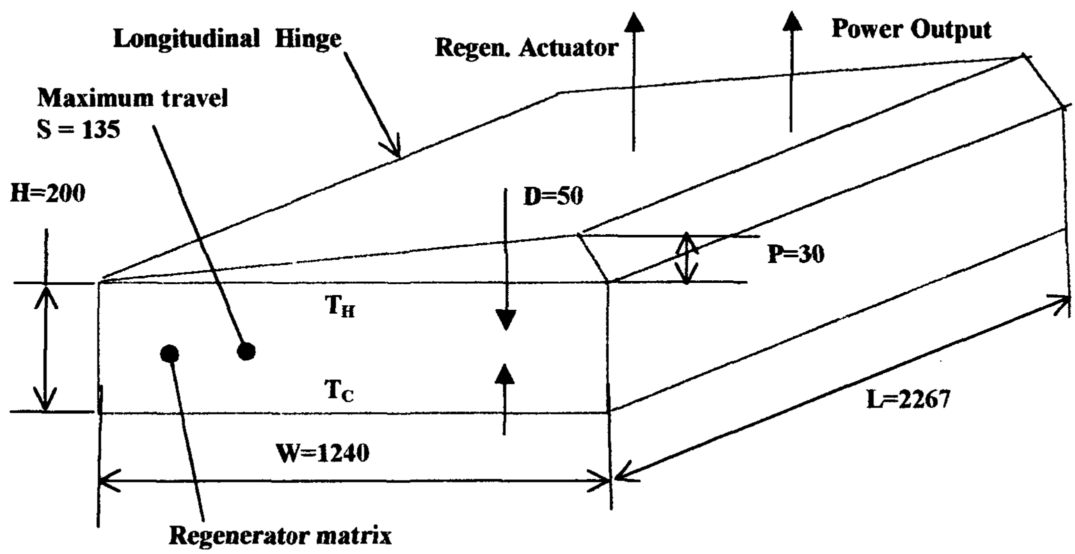

Figure F.1: Diagrammatic Representation of One Machine Panel

NOMENCLATURE AND ASSUMPTIONS

Consider the engine, shown diagrammatically in figure F.2, having constant dead spaces at both hot and cold ends, together with a volume variation at the hot end due to the displacement of the hinged cover.

Here:

V_R : total constant space occupied by regenerator (T_R)

εV_R : constant regenerator void volume (T_R)

ε : void fraction

V_C : variable cold-space volume (T_C)

$V_{C\,max}$: maximum cold-space volume due to displacer motion (T_C)

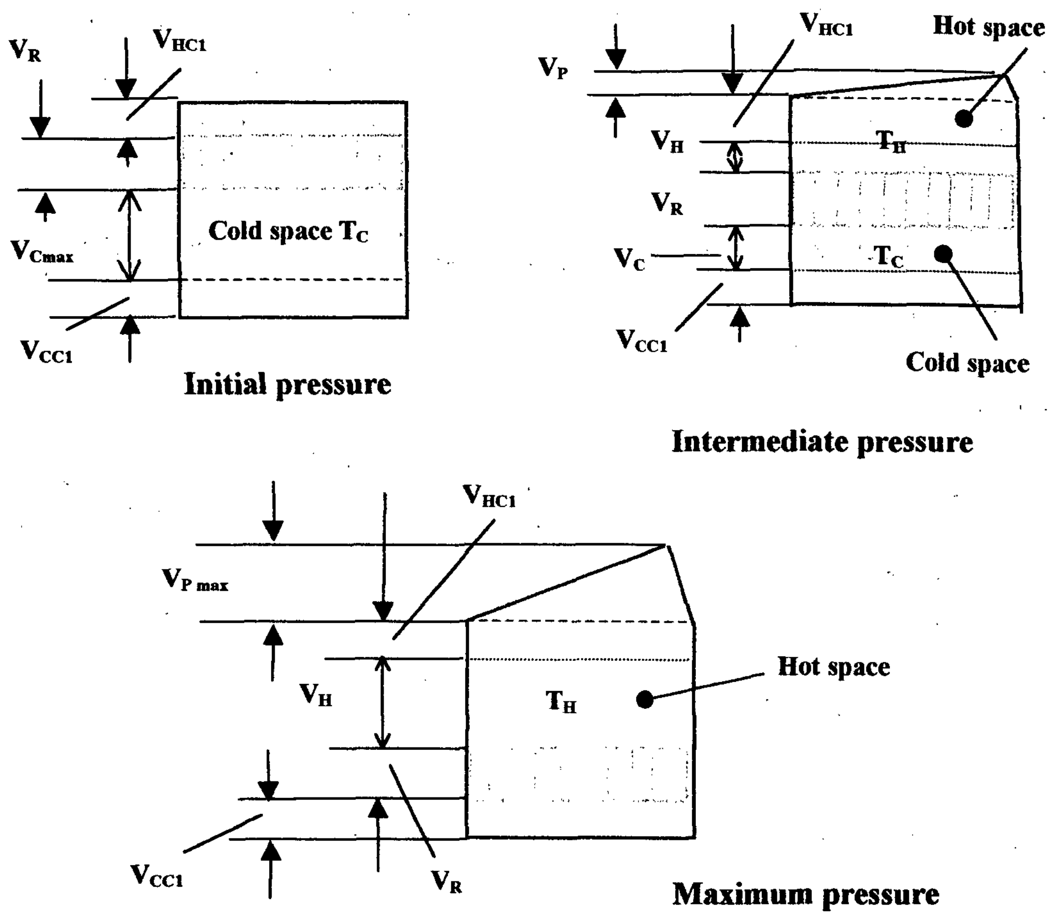

Figure F.2: Diagrammatic Representation of Engine

V_{CCl}	: cold-space clearance volume (T_C)
V_p	: variable 'piston' volume (T_H)
$V_{p\,max}$	: maximum piston volume (T_H)
V_H	: variable hot-space volume (T_H)
$V_{H\,max}$	: maximum hot-space volume due to displacer motion (T_H)
V_{HCl}	: constant volume hot-space clearance volume (T_H)
T_H	: constant hot-end temperature
T_R	: constant regenerator mean temperature

T_C : constant cold-end temperature

m_H : total hot-space mass = $m_{HCl} + m_p + m_H$

m_R : variable mass of working fluid in regenerator

m_C : total cold-space mass = $m_{CCl} + m_C$

p : uniform system pressure, i.e, no pressure gradients within the system

p_{min} : minimum system pressure

p_{max} : maximum system pressure

ASSUMPTIONS

- There are no pressure gradients within the system at all times, i.e, $p = p_C = p_R = p_H$
- The total volume occupied by the working fluid is, $V_{tot} = V_p + V_{HCl} + V_H + \varepsilon V_R + V_C + V_{CCl}$ where ε is the void fraction of the regenerator
- The mass of the working fluid in the system is constant, i.e., $m_{tot} = m_p + m_{HCl} + m_H + m_R + m_C + m_{CCl}$ where m_R is the mass of the working fluid in the regenerator void volume. Here m_p , m_{HCl} and m_H are at T_H, m_R is at T_R, and m_C and m_{CCl} are at T_C. That is, the temperature of the working fluid in all hot spaces is constant at T_H and that in the two cold spaces is constant at T_C
- The temperature distribution in the regenerator is linear with the hot-end temperature $T_{rH} = T_H$ and the cold-end temperature $T_{rC} = T_C$. The mean regenerator temperature is thus $T_R = (T_H - T_C) / \ln (T_H / T_C)$ and is constant.
- The ideal gas equation of state is $pV = mRT$

IDEALIZED METHOD OF OPERATION OF THE ENGINE

Thermodynamic analysis of the Wagner solar-powered Stirling-type engine can be carried out at three levels of complexity: first-order or quasi-static; second-order or lumped parameter; and third-order or dynamic numerical simulation.

For the purpose of this report it was considered adequate to use a first-order model which could provide information on the effects of various parameters, such as dead space volumes, initial or minimum cycle pressures and the like. These results could then be combined with the heat transfer predictions presented in Appendices A to E, to establish operating domains and optimum values.

Thermodynamic analysis of cycle requires determination of the state points at the start and end of each process as well as the paths followed in going from one state point to the next. The usual method of representing such cycles is by pressure/volume diagrams such as that shown in figure F.3(b). Such diagrams have the advantage that the area contained within the closed cycle is proportional to the work done per cycle.

In order to keep the analysis simple it is convenient to subdivide the cycle as depicted in Figs F.3 (a & b). These are idealizations of the real processes. Also since the pressure excursions during each process are relatively small it is convenient at this stage to treat the paths followed during each process as straight lines on pV plots.

In Fig F.3 (a) the cycle has been subdivided into four discrete processes. The resultant plots on pressure/volume coordinate is shown in Fig F.3 (b). Here the volume coordinate is taken as $V = V_p + V_H + V_{HCl}$. As we are only concerned with the state point values we can determine these by assuming that the displacer / regenerator and the hinged panel ('piston') change in discret steps. Note that it is assumed that the gas temperature in the hot clearance volume is equal to that in the hot space. Similarly the cold clearance volume temperature is the same as that in the cold space. Also note that $V_{H\,max} = V_{C\,max}$.

ANALYSIS

For mass conservation

$$m_{tot} = m_p + m_{HCl} + m_H + m_R + m_C + m_{CCl}$$

and substituting from the equation of state

$$pV = mRT$$

$$m_{tot} = \frac{pV_P}{RT_H} + \frac{pV_{HCl}}{RT_H} + \frac{pV_H}{RT_H} + \frac{p\varepsilon V_R}{RT_R} + \frac{pV_C}{RT_C} + \frac{pV_C}{RT_C}$$

$$= \frac{p}{R}\left[\frac{V_H + V_{HCl} + V_H}{T_H} + \frac{\varepsilon V_R}{T_R} + \frac{V_C + V_{CCl}}{T_C}\right]$$

At state point 1:

$$p = p_1;\ V_p = V_{pmax}; V_H = 0; V_{HCl} = V_{CCl}; V_C = V_{C\max},$$

hence

$$m_{tot} = \frac{p_1}{R}\left[\frac{V_{p\,max} + V_{HCl}}{T_H} + \frac{\varepsilon V_R}{T_R} + \frac{V_{C\,max} + V_{CCl}}{T_C}\right] \qquad (1)$$

Thus since all the terms on the RHS are known m_{tot} is known, hence

$$p = \frac{m_{tot}R}{\left[\frac{V_P + V_H + V_{HCl}}{T_H} + \frac{\varepsilon V_R}{T_R} + \frac{V_C + V_{CCl}}{T_C}\right]} \qquad (2)$$

Hence the work done during each process is given by

$$W = p\ \Delta V_p$$

1

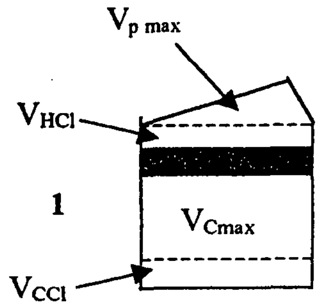

$$V_p=V_{p\,max}\,;\; V_H=0\,;\; V_C = V_{C\,max}\,;\; V_{HCl} = V_{CCl}$$

$$p_1 = \frac{m_{tot}R}{\left[\dfrac{V_{p\,max}+V_{HCl}}{T_H}+\dfrac{\varepsilon V_R}{T_R}+\dfrac{V_{C\,max}+V_{CCl}}{T_C}\right]} \qquad (3)$$

2

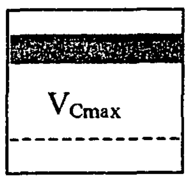

$$V_p=0\,;\; V_H=0\,;\; V_C = V_{C\,max}\,;\; V_{HCl} = V_{CCl}$$

$$p_2 = \frac{m_{tot}R}{\left[\dfrac{V_{HCl}}{T_H}+\dfrac{\varepsilon V_R}{T_R}+\dfrac{V_{C\,max}+V_{CCl}}{T_C}\right]} \qquad (4)$$

3

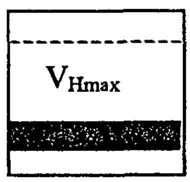

$$V_p=0\,;\; V_H=V_{H\,max}\,;\; V_C =0\,;\; V_{HCl} = V_{CCl}$$

$$p_3 = \frac{m_{tot}R}{\left[\dfrac{V_{H\,max}+V_{HCl}}{T_H}+\dfrac{\varepsilon V_R}{T_R}+\dfrac{V_{CCl}}{T_C}\right]} \qquad (5)$$

4

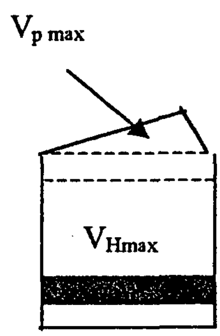

$$V_p=V_{p\,max}\,;\; V_H=V_{H\,max}\,;\; V_C =0\,;\; V_{HCl} = V_{CCl}$$

$$p_4 = \frac{m_{tot}R}{\left[\dfrac{V_{p\,max}+V_{H\,max}+V_{HCl}}{T_H}+\dfrac{\varepsilon V_R}{T_R}+\dfrac{V_{CCl}}{T_C}\right]} \qquad (6)$$

Figure F.3 (a) : State Point Pressures

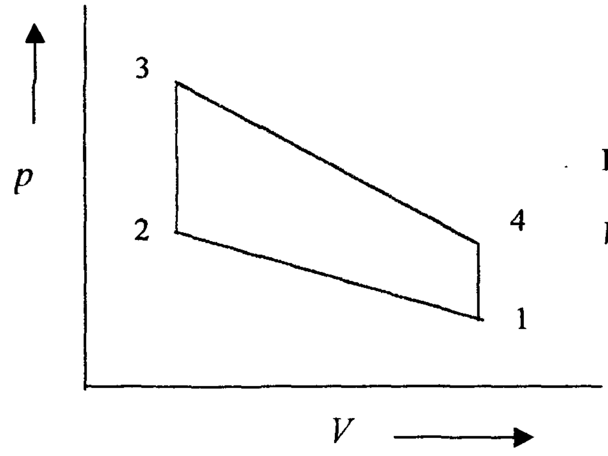

Here

$V = V_p + V_H + V_{HCl}$

Figure F.3 (b): *pV* Diagram

For $1 \rightarrow 2$

$$W_{12} = -p_{mean}V_{pmax} = -\left(\frac{p_1 + p_2}{2}\right)V_{pmax}$$

For $2 \rightarrow 3$

$$W_{23} = 0$$

For $3 \rightarrow 4$

$$W_{34} = p_{mean}V_{pmax} = \left(\frac{p_3 + p_4}{2}\right)V_{p\max}$$

Hence for the cycle

$$W_{cycle} = \left[\left(\frac{p_3 + p_4}{2}\right) - \left(\frac{p_1 + p_2}{2}\right)\right]V_{pmax} \qquad (7)$$

The power developed per panel

$$P_1 = f\ W_{cycle}$$

or for the two panels

$$P_T = 2P_1$$

NUMERICAL EXAMPLES

Given:

$W = \mathbf{1240}$ mm; $L = \mathbf{2257}$ mm; $H = \mathbf{200}$ mm; $D = \mathbf{50}$ mm; $T_H = \mathbf{388}$ K; $T_C = \mathbf{308}$ K;

$p_{ambient} = \mathbf{101}$ kPa; $T_R = (T_H - T_C)/ln(T_H / T_C)$; $V_{pmax} = \mathbf{0.5}\,WLD$; frequency

$f = \mathbf{0.5}$ cycle/sec; regenerator stroke length $S = \mathbf{135}$ mm; specific gas constant

for air $R = \mathbf{287}$ J/kg K; void fraction $\varepsilon = 0.6$.

Find:

Work done per cycle for each panel; indicated power for the whole machine (2 panels)

Assumptions:

As specified in section 'Nomenclature and Assumptions'

• Solution 1 - Original engine

The total internal volume of a panel with the cover down is

$$V_{sys(down)} = WLH = (\mathbf{1240})(\mathbf{2257})(\mathbf{200}) = \mathbf{0.5597}\ \text{m}^3$$

$$V_{HCl} = V_{CCl} = 0.5\,WL(H - S) = (0.5)(1240)(2257)(200 - 135) = 0.09096 \text{ m}^3$$

$$V_R = WLD = (1240)(2257)(50) = 0.1399 \text{ m}^3$$

$$\varepsilon V_R = (0.6)(0.1399) = 0.08396 \text{ m}^3$$

$$V_{pmax} \approx 0.5\,WPL = (0.5)(1240)(30)(2257) \approx 0.04198 \text{ m}^3$$

Total internal volume of panel with cover up

$$V_{sys(up)} = 0.5597 + 0.04198 = 0.60168 \text{m}^3$$

The total volume of working fluid in the system

$$V_f = V_{sys(up)} - (1 - \varepsilon)V_R = V_{pmax} + \varepsilon V_R + 2V_{HCl} + V_{Cmax}$$

hence

$$V_{sys(up)} = V_{pmax} + 2V_{HCl} + V_{Cmax} + V_R$$

and

$$V_{Cmax} = V_{sys(up)} - V_{pmax} - V_R - 2V_{HCl} = V_{H\max} = 0.60168 - 0.04198 - 0.1399 - 0.18192$$

$$= 0.2379 \text{ m}^3$$

also

$$T_R = (388 - 308)ln(388/308) = 346.5 \text{ K}$$

hence

$$m_{tot} = \frac{p_1}{R}\left[\frac{V_{pmx} + V_{HCl}}{T_H} + \frac{\varepsilon V_R}{T_R} + \frac{V_{C\max} + V_{CCl}}{T_C}\right]$$

$$= \frac{(101)(10^3)}{(287)}\left[\frac{0.04198 + 0.09096}{388} + \frac{0.08396}{346.5} + \frac{0.2379 + 0.09096}{308}\right]$$

$$= (351.9)(3.4263 + 2.4231 + 10.6773)(10^{-4}) = (351.9)(16.5267)(10^{-4})$$

$$= 0.5816 \text{ kg}$$

Thus from equ (4)

$$p_2 = \frac{(0.5816)(287)}{\left[\frac{0.09096}{388} + \frac{0.08396}{346.5} + \frac{0.2379 + 0.09096}{308}\right]}$$

$$= \frac{166.92}{[2.3443 + 2.4231 + 10.6773](10^{-4})} = \frac{166.92}{(15.445)(10^{-4})} = 108.1 \text{ kPa}$$

From equ (5)

$$p_3 = \frac{166.92}{\frac{0.2379 + 0.09096}{388} + (2.4231)(10^{-4}) + \frac{0.09096}{308}}$$

$$= \frac{166.92}{[8.4758 + 2.4231 + 2.9532](10^{-4})} = \frac{166.92}{(13.852)(10^{-4})} = 120.5 \text{ kPa}$$

$$p_4 = \frac{166.92}{\left[\frac{0.04198 + 0.2379 + 0.09096}{388} + (2.4231)(10^{-4}) + \frac{0.09096}{308}\right]}$$

$$= \frac{166.92}{[9.5577 + 2.4231 + 2.9532](10^{-4})} = \frac{166.92}{(14.934)(10^{-4})} = 111.8 \text{ kPa}$$

hence

$$W_{cycle} = [(p_3 + p_4) - (p_1 + p_2)]V_{pmax}/2 = [(120.5 + 111.8) - (101 + 108.1)](10^3)(0.04198)/2$$

$$= [232.3 - 209.1](10^3)(0.04198)/2 = (23.2)(10^3)(0.04198)/2 = 487.0 \text{ Nm}$$

and the power developed per panel at a frequency $f = 0.5$ cycles per second

$$P_1 = (487)(0.5) = 243.5 \text{ Watts}$$

or with both panels

$$P_2 = 487 \text{ Watts}$$

• Solution 2 - Original engine with zero clearances and unchanged regenerator stroke

If there are no clearance, ie, $V_{HCl} = V_{CCl} = 0$ and $V_{p\ max}$, $V_{H\ max}$ and $V_{C\ max}$ remain the same then from equ (1)

$$m_{tot} = \frac{p_1}{R}\left[\frac{V_{pmx}}{T_H} + \frac{\varepsilon V_R}{T_R} + \frac{V_{Cmax}}{T_C}\right] = \frac{(101)(10^3)}{(287)}\left[\frac{0.04198}{388} + \frac{0.08396}{346.5} + \frac{0.2379}{308}\right]$$

$$= (351.9)(1.08196 + 2.4231 + 7.7240)(10^{-4}) = (351.9)(11.2291)(10^{-4})$$

$$= 0.3952 \text{ kg}$$

then from equ(4)

$$p_2 = \frac{m_{tot}R}{\dfrac{\varepsilon V_R}{T_R} + \dfrac{V_{C\max}}{T_C}} = \frac{(0.3952)(287)}{(2.4281 + 7.7240)(10^{-4})} = \frac{113.4}{(10.1471)(10^{-4})} = 111.8 \text{ kPa}$$

From equ (5)

$$p_3 = \frac{m_{tot}R}{\frac{V_{H\max}}{T_H} + \frac{\varepsilon V_R}{T_R}} = \frac{113.4}{\frac{0.2379}{388} + \frac{0.08396}{346.5}} = \frac{113.4}{(6.1314 + 2.4231)(10^{-4})} = \frac{113.4}{(8.5545)(10^{-4})}$$

$$= 132.6 \text{ kPa}$$

and from equ (6)

$$p_4 = \frac{m_{tot}R}{\frac{V_{p\max} + V_{H\max}}{T_H} + \frac{\varepsilon V_R}{T_R}} = \frac{113.4}{(1.08196 + 2.4231)(10^{-4})} = \frac{113.4}{(9.6365)(10^{-4})} = 117.7 \text{ kPa}$$

Thus

$$W_{cycle} = [(p_3 + p_4) - (p_1 + p_2)]V_{p\max}/2$$

$$= [250.2 - 212.8](10^3)(0.04198)/2 = 786.71 \text{ Nm}$$

and

$$P_1 = (0.5)(786.7) = 393.4 \text{ Watts}$$

thus

$$P_2 = 786.7 \text{ Watts}$$

- **<u>Solution 3 - Original engine with zero clearance and increased regenerator stroke</u>**

If the clearances V_{HCl} and V_{CCl} were incorporated into V_H and V_C by increasing the regenerator stroke volume then

$$V'_{H\,max} = V_{H\,max} + V_{HCl} = V_{C\,max} + V_{CCl} = V'_{C\,max}$$

$$= 0.2379 + 0.09096 = 0.3289 \text{ m}^3$$

In this case

$$m_{tot} = \frac{p_1}{R}\left[\frac{V_{p\,max}}{T_H} + \frac{\varepsilon V_R}{T_R} + \frac{V'_{C\,max}}{T_C}\right] = \frac{(101)(10^3)}{(287)}\left[\frac{0.04198}{388} + \frac{0.08396}{346.5} + \frac{0.3284}{308}\right]$$

$$= (351.9)(14.1823)(10^{-4}) = 0.4991 \text{ kg}$$

Thus from equ (4)

$$p_2 = \frac{(0.4991)(287)}{[2.4231 + 10.6773](10^{-4})} = \frac{143.24}{(13.1004)(10^{-4})} = 109.3 \text{ kPa}$$

From equ (5)

$$p_3 = \frac{143.24}{\frac{0.3289}{388} + (2.4231)(10^{-4})} = \frac{143.24}{(8.4758 + 2.4231)(10^{-4})} = \frac{143.24}{(10.8989)(10^{-4})}$$

$$= 131.4 \text{ kPa}$$

Fron equ (6)

$$p_4 = \frac{143.24}{\frac{0.04198 + 0.3289}{388} + (2.4231)(10^{-4})} = \frac{143.24}{(9.5577 + 2.4231)(10^{-4})}$$

$$= \frac{143.24}{(11.9808)(10^{-4})} = 119.6 \text{ kPa}$$

Hence

$$W_{cycle} = [(p_3 + p_4) - (p_1 + p_2)]V_{pmax} / 2$$

$$= [(131.4 + 119.6) - (101 + 109.3)](10^3)(0.04198)/2$$

$$= (407)(10^3)(0.04198)/2 = 854.3 \text{ Nm}$$

Thus

$$P_1 = (0.5)(854.3) = 427 \text{ Watts}$$

and

$$P_2 = 854 \text{ Watts}$$

- **<u>Solution 4 - Original engine with clearances, unchanged regenerator stroke and initial pressure of 202 kPa</u>**

Here

$$m_{tot} = (2)(0.5816) = 1.1632 \text{ kg}$$

$$p_2 = (2)(108.1) = 216.2 \text{ kPa}$$

$$p_3 = (2)(120.5) = 241 \text{ kPa}$$

$$p_4 = (2)(111.8) = 223.6 \text{ kPa}$$

$$W_{cycle} = 974 \text{ Nm}$$

$$P_1 = (0.5)(974) = 487 \text{ Watts}$$

$$P_2 = (2)(487) = 974 \text{ Watts}$$

SUMMARY AND CONCLUSIONS

TABLE F.1 : Summary of Results

RESULTS → *DESCRIPTION ↓*	m_{tot} [kg]	p_1 [kPa]	p_2 [kPa]	p_3 [kPa]	p_4 [kPa]	W [J]	P_1 [W]	P_2 [W]
Original engine with clearance	0.582	101	108.1	120.5	111.8	487	244	487
Original with no clearance	0.395	101	111.8	132.6	117.7	787	393	787
Increased regenerator stroke	0.499	101	109.3	131.4	119.6	854	427	853
Minimum cycle pressure	1.1632	202	216.2	241.0	223.6	974	487	974

Table F.1 above summarizes the performance of the Wagner engine under sets of different conditions. These were selected to give an indication of the sensitivity of this engine to clearance volumes, regenerator stroke length and minimum cycle pressures. Some of the parameters still to be explored include effects of working fluid leakage, flexibility of cover framework, thickness of the regenerator/displacer matrix, temperature gradients in both the hot and cold spaces, mechanical losses, and the like. This should be followed by a refinement of the present model and optimization of the resultant operating parameters.

Of all the cases analyzed the present engine yielded the lowest power output. The effect of eliminating the clearances of both the hot and cold spaces but still using the same regenerator stroke volume - that is by moving the lower surface of the cold space up and that of the hot space down - although significantly reducing the mass of the working fluid nevertheless increased the power output from 487 Watts to 787 Watts, that is, an increase of some 62 per cent. Eliminating the cold and hot clearance volumes by increasing the regenerator stroke volume increased the power output of the existing engine from 487 Watts to 853 Watts, an increase of some 75 per cent, even though the mass of the working fluid was then reduced from 0.582 kg to 0.499 kg - a drop of about 14 per cent.

The last case considered was with the same clearances and regenerator stroke volumes as the present engine but with double the initial pressure. Clearly the power developed is directly proportional to the initial cycle pressure, or more strictly the total working fluid mass. However increasing the pressure will increase the leakage of the working fluid which will lower the power developed.

The flexibility of the top cover and seal also contributes to diminishing the output power by, in effect, behaving as a variable clearance volume. Even assuming that the resultant deflection is elastic, the energy stored at the higher cycle pressure would only be recovered at lower cycle pressures resultimg in an overall power loss.

Finally it must be reiterated that the model used for the thermodynamic analysis is based on a significant number of approximations all of which have the effect of over-predicting the engine performance. Even without taking the effects of leakage, cover flexibility and heat losses into account it is anticipated that the power developed by a real machine is unlikely to be greater than about 50 per cent of that predicted by the model used.

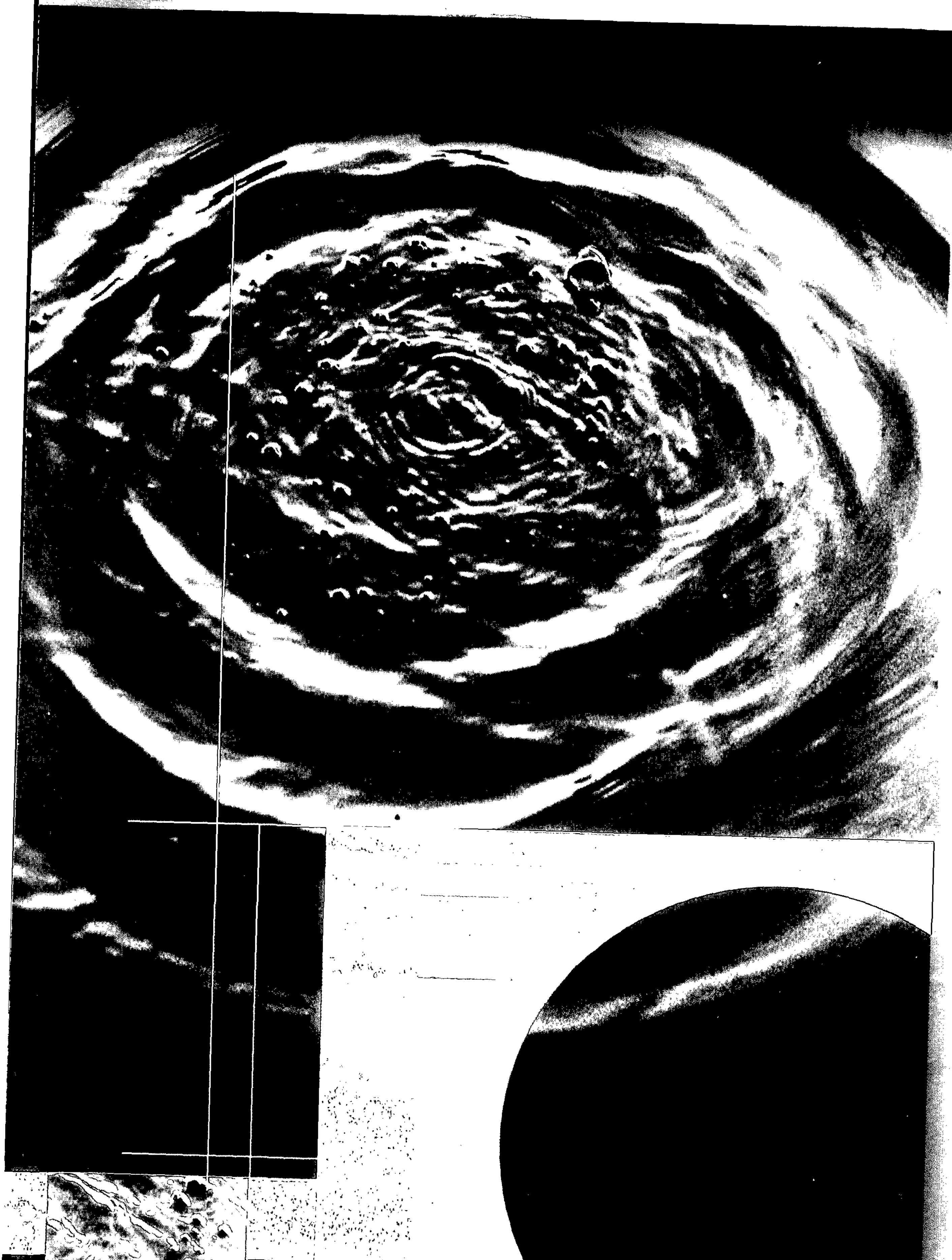

Water Research Commission

PO Box 824, Pretoria, 0001, South Africa

Tel: +27 12 330 0340, Fax: +27 12 331 2565

Web: http://www.wrc.org.za